Efficient methods for computing ground states of spin-1 Bose-Einstein condensates based on their characterizations

Weizhu Bao[*], I-Liang Chern[†], Yanzhi Zhang[‡]

Abstract

In this paper, we propose efficient numerical methods for computing the ground states of spin-1 Bose-Einstein condensates (BECs) with/without the Ioffe-Pritchard magnetic field $B(\mathbf{x})$. When $B(\mathbf{x}) \neq 0$, a numerical method is introduced to compute the ground states and applied to study properties of the ground states. Numerical results suggest that the densities of $m_F = \pm 1$ components in the ground states are identical for any nonzero $B(\mathbf{x})$. In particular, if $B(\mathbf{x}) \equiv B$ is a constant, the ground states satisfy the single-mode approximation. When $B(\mathbf{x}) \equiv 0$, efficient and simpler numerical methods are presented to solve the ground states of spin-1 BECs based on their ferromagnetic/antiferromagnetic characterizations. Numerical simulations show that our methods are more efficient than those in the literature. In addition, some conjectures are made from our numerical observations.

Keywords: Spin-1 Bose-Einstein condensate; Ground state; Ferromagnetic; Antiferromagnetic; Single-mode approximation.

1 Introduction

{*section1*}

Since its first realization in 1995, Bose–Einstein condensation (BEC) has become an important tool to study behaviors of quantum many-body systems. In earlier BEC experiments, the atoms were confined in a magnetic trap, where their spin degree of freedom was frozen [1, 11]. Recently, the development of optical trapping techniques has enabled to confine atoms independently of their spin orientation and thus result in so-called spinor condensates. The spinor BEC has revealed numerous exciting new phenomena which are not possessed by single-component (spin-frozen) condensates. It has provided a unique possibility of exploring fundamental concepts of quantum mechanics in a remarkably controllable and tunable environment [28, 29, 27].

In the mean-field approximation, a spin-F ($F \in \mathbb{N}$) condensate can be described by coupled Gross-Pitaevskii equations (GPEs) consisting of $2F+1$ equations, each of which governs one of the $2F+1$ hyperfine states ($m_F = -F, -F+1, \ldots, F-1, F$). For a spin-1

[*]Department of Mathematics and Center for Computational Science and Engineering, National University of Singapore, Singapore 119076 (bao@math.nus.edu.sg).

[†]Department of Applied Mathematics and Center of Mathematical Modeling and Scientific Computing, National Chiao Tung University, Hsinchu, 30010, Taiwan (chern@math.nctu.edu.tw).

[‡]Department of Mathematics and Statistics, Missouri University of Science and Technology, Rolla, MO 65409-0020, USA (Corresponding author, zhangyanz@mst.edu).

BEC, the three component dimensionless GPEs have the following form [7, 5, 6, 28]:

$$\begin{aligned} i\partial_t\psi_1(\mathbf{x},t) &= \left(H+\beta_s(|\psi_1|^2+|\psi_0|^2-|\psi_{-1}|^2)\right)\psi_1+\beta_s\psi_0^2\psi_{-1}^*+B\psi_0, \\ i\partial_t\psi_0(\mathbf{x},t) &= \left(H+\beta_s(|\psi_1|^2+|\psi_{-1}|^2)\right)\psi_0+2\beta_s\psi_1\psi_0^*\psi_{-1}+B^*\psi_1+B\psi_{-1}, \\ i\partial_t\psi_{-1}(\mathbf{x},t) &= \left(H+\beta_s(|\psi_{-1}|^2+|\psi_0|^2-|\psi_1|^2)\right)\psi_{-1}+\beta_s\psi_1^*\psi_0^2+B^*\psi_0, \end{aligned} \quad (1.1) \quad \{GPEs\}$$

where $\psi_j(\mathbf{x},t)$ is the complex-valued wave function of the j-th ($j=1,0,-1$) component with $\mathbf{x}\in\mathbb{R}^d$ (for $d=1,2,3$) and $t\geq 0$. The operator H is defined by

$$H=-\frac{1}{2}\nabla^2+V_d(\mathbf{x})+\beta_n\sum_{j=-1}^{1}|\psi_j|^2, \quad (1.2) \quad \{Hoperator\}$$

where $V_d(\mathbf{x})$ represents the external trapping potential and it is determined by the type of system under investigation. For instance, if a three-dimensional (3D) harmonic potential is considered, it takes the form $V_3(\mathbf{x})=\frac{1}{2}(\omega_x^2x^2+\omega_y^2y^2+\omega_z^2z^2)$ with ω_x, ω_y and ω_z being the dimensionless trapping frequencies in x-, y- and z-directions, respectively. The constants β_n and β_s describe the spin-independent interaction and spin-dependent exchange interaction, respectively, and they are proportional to N, the total number of atoms in the condensate. When $\beta_n>0$ (resp. <0), the spin-independent interaction is repulsive (resp. attractive); while $\beta_s>0$ (resp. <0), the spin-exchange interaction is antiferromagnetic (resp. ferromagnetic). The dimensionless function $B(\mathbf{x})\in\mathbb{C}$ represents the external Ioffe-Pritchard magnetic field [12, 14, 16]. In addition, f^* represents the conjugate of the function f.

There are two important invariants of (1.1): the *normalization of the wave functions*,

$$\|\Psi(\cdot,t)\|^2=\sum_{j=-1}^{1}\|\psi_j(\cdot,t)\|^2:=\sum_{j=-1}^{1}\int_{\mathbb{R}^d}|\psi_j(\mathbf{x},t)|^2d\mathbf{x}\equiv\|\Psi(\cdot,0)\|^2=1, \quad t\geq 0, \quad (1.3) \quad \{Normal\}$$

with $\Psi(\mathbf{x},t)=(\psi_1(\mathbf{x},t),\psi_0(\mathbf{x},t),\psi_{-1}(\mathbf{x},t))^T$, and the *energy*

$$E(\Psi(\cdot,t)):=E_0(\Psi(\cdot,t))+2\mathrm{Re}\left(\int_{\mathbb{R}^d}B(\psi_1^*\psi_0+\psi_0^*\psi_{-1})d\mathbf{x}\right)\equiv E(\Psi(\cdot,0)), \quad t\geq 0, \quad (1.4) \quad \{energy\}$$

with $\mathrm{Re}(f)$ denoting the real part of the function f and

$$\begin{aligned} E_0(\Psi(\cdot,t)):=\int_{\mathbb{R}^d}\Bigg[&\sum_{j=-1}^{1}\left(\frac{1}{2}|\nabla\psi_j|^2+V_d(\mathbf{x})|\psi_j|^2\right)+\frac{\beta_n}{2}\left(|\psi_1|^2+|\psi_0|^2+|\psi_{-1}|^2\right)^2 \\ &+\frac{\beta_s}{2}\left(|\psi_1|^2-|\psi_{-1}|^2\right)^2+\beta_s|\psi_0|^2\left(|\psi_1|^2+|\psi_{-1}|^2\right)+2\beta_s\mathrm{Re}\left(\psi_1^*\psi_0^2\psi_{-1}^*\right)\Bigg]d\mathbf{x}, \end{aligned} \quad (1.5) \quad \{energy0\}$$

for $t\geq 0$, i.e., $E_0(\Psi(\cdot,t))$ represents the energy when $B(\mathbf{x})\equiv 0$. Furthermore, in the case of $B(\mathbf{x})\equiv 0$, the *total magnetization* is also conserved, i.e.,

$$M(\Psi(\cdot,t)):=\int_{\mathbb{R}^d}\left(|\psi_1(\mathbf{x},t)|^2-|\psi_{-1}(\mathbf{x},t)|^2\right)d\mathbf{x}\equiv M(\Psi(\cdot,0))=M, \quad t\geq 0, \quad (1.6) \quad \{Magnetic\}$$

with $-1\leq M\leq 1$.

Among all stationary states, ground states which have the lowest energy play an important role in understanding the properties of BECs. There have been many studies on ground states of spin-1 condensates. In [26], the phase diagram of the ground states of spin-1 BECs was first reported in the Thomas-Fermi regime. The phenomena of broken axisymmetry phase were observed in [23] for a spin-1 ferromagnetic condensate. Recently, Matuszewski et al. compared the phase separation of the ground states in the ferromagnetic and antiferromagnetic systems [19, 20]. Cao et al. proved the existence of the ground states in one-dimensional condensates [8]. On the other hand, some numerical methods have been proposed in recent literatures to compute the ground states of spin-1 BECs in the absence of the external Ioffe-Pritchard magnetic field (i.e., $B(\mathbf{x}) \equiv 0$ in (1.1)). For instance, Bao and Wang presented a continuous normalized gradient flow (CNGF) and constructed a Crank-Nicolson finite difference scheme to discretize it [5]. To improve the computational efficiency of the method in [5], later Bao and Lim introduced a gradient flow with discrete normalization (GFDN) to replace the CNGF, where an addition normalization condition was imposed [6, 17]. Chen et al. proposed a pseudo-arclength continuation method to compute the ground states of spin-1 BECs [9]. To the best of our knowledge, all these methods focus on computing the ground states of spin-1 BECs where $B(\mathbf{x}) = 0$ and so far there are still no numerical reports about the ground states when $B(\mathbf{x}) \neq 0$. In addition, to obtain the ground states in the cases of $B(\mathbf{x}) = 0$, all the available methods solve three-component GPE type equations, which makes the simulations very costly. Note that when $B(\mathbf{x}) = 0$, the ground states of spin-1 BECs can be simplified to a single-mode (resp. two-component) reduction for ferromagnetic (resp. antiferromagnetic) systems [15, 30, 18]. Thus, in this case the ground states can be effectively found by solving the reduced single or two-component systems instead of the original three-component one. In this paper, we aim to propose i) a numerical method for computing ground states of spin-1 BECs when $B(\mathbf{x}) \neq 0$; ii) efficient and simpler methods for the case of $B(\mathbf{x}) \equiv 0$, by taking into account their ferromagnetic and antiferromagnetic characterizations.

This paper is organized as follows. In Section 2, we propose a numerical method for the case when the Ioffe-Pritchard magnetic field $B(\mathbf{x}) \neq 0$. While when $B(\mathbf{x}) \equiv 0$, the ground states of the three-component system (1.1) are characterized by those of the corresponding reduced systems, i.e., the single-mode and two-component reductions for the ferromagnetic and antiferromagnetic condensates, respectively. The reductions of the ground states for ferromagnetic and antiferromagnetic spin-1 BECs are discussed in Section 3, followed by their numerical discretizations. Numerical results of ground states as well as comparison between different methods are presented in Section 4. In Section 5, we draw some conclusions and conjectures based on our numerical observations.

2 Numerical methods for ground states with nonzero B

{*section2*}

In this section, we study the ground states of spin-1 BECs with an Ioffe-Pritchard magnetic field, i.e., $B(\mathbf{x}) \neq 0$ in (1.1). Some numerical methods have been recently proposed in the literature [5, 6, 17, 9] to compute the ground states of spin-1 BECs in the absence of $B(\mathbf{x})$. However, there is still no numerical report on the ground states when $B(\mathbf{x}) \neq 0$.

When $B(\mathbf{x}) \neq 0$, the ground state $\Phi_g(\mathbf{x}) = (\phi_{1,g}(\mathbf{x}), \phi_{0,g}(\mathbf{x}), \phi_{-1,g}(\mathbf{x}))^T$ is defined by minimizing the energy functional E in (1.4) subject to the normalization of the wave func-

tions, i.e.,

Find $(\Phi_g \in S)$, such that

$$E_g := E(\Phi_g) = \min_{\Phi \in S} E(\Phi), \tag{2.1}$$ {*minimizer6*}

where the set S is defined by

$$S := \left\{ \Phi = (\phi_1,\, \phi_0,\, \phi_{-1})^T \,|\, \|\Phi\|^2 = 1,\; E(\Phi) < \infty \right\}.$$

It is easy to see that the ground state Φ_g defined in (2.1) satisfies the following Euler-Lagrange equations

$$\begin{aligned}
\mu\phi_1(\mathbf{x}) &= \left(H + \beta_s(|\phi_1|^2 + |\phi_0|^2 - |\phi_{-1}|^2)\right)\phi_1 + \beta_s\,\phi_0^2\phi_{-1}^* + B\phi_0, \\
\mu\phi_0(\mathbf{x}) &= \left(H + \beta_s(|\phi_1|^2 + |\phi_{-1}|^2)\right)\phi_0 + 2\beta_s\,\phi_1\phi_0^*\phi_{-1} + B^*\phi_1 + B\phi_{-1}, \\
\mu\phi_{-1}(\mathbf{x}) &= \left(H + \beta_s(|\phi_{-1}|^2 + |\phi_0|^2 - |\phi_1|^2)\right)\phi_{-1} + \beta_s\,\phi_1^*\phi_0^2 + B^*\phi_0,
\end{aligned} \tag{2.2}$$ {*SGPEs-B*}

with the constraint

$$\|\Phi\|^2 = \int_{\mathbb{R}^d} \left(|\phi_1(\mathbf{x})|^2 + |\phi_0(\mathbf{x})|^2 + |\phi_{-1}(\mathbf{x})|^2\right) d\mathbf{x} = 1, \tag{2.3}$$ {*constraint6*}

where the operator H is defined in (1.2). The eigenvalue μ is the Lagrange multiplier (or called as chemical potential) corresponding to the constraint in (2.3), which can be computed from its eigenfunction Φ by

$$\begin{aligned}
\mu = \mu(\Phi) = E(\Phi) + \int_{\mathbb{R}^d} \Bigg[&\frac{\beta_n}{2}\left(|\phi_1|^2 + |\phi_0|^2 + |\phi_{-1}|^2\right)^2 + \frac{\beta_s}{2}\left(|\phi_1|^2 - |\phi_{-1}|^2\right)^2 \\
&+\beta_s|\phi_0|^2\left(|\phi_1|^2 + |\phi_{-1}|^2\right) + 2\beta_s \mathrm{Re}\left(\phi_1^*\phi_0^2\phi_{-1}^*\right)\Bigg] d\mathbf{x}.
\end{aligned}$$

In fact, the system in (2.2) can also be obtained from the time-dependent GPEs in (1.1) by substituting the ansatz

$$\psi_j(\mathbf{x}, t) = e^{-i\mu t}\,\phi_j(\mathbf{x}), \qquad j = 1, 0, -1. \tag{2.4}$$ {}

The eigenfunctions Φ of the constrained nonlinear eigenvalue problem (2.2)–(2.3) are usually called as *stationary states* of spin-1 BECs. Among all stationary states, the eigenfunction with minimum energy is called as the *ground state* and those with larger energies are usually called as *excited states*.

Various algorithms have been proposed in the literature to find the minimizer of the energy functional under constraints. While the imaginary time method (i.e., replacing t with $-i\tau$ in (1.1)) is one of the most popular approaches in studying the ground states of BECs. It is mathematically justified by the normalized gradient flow [10, 2]. In this paper, we will develop our numerical methods for computing ground states of spin-1 BECs based on the discretized normalized gradient flow; see more information in [2]. Choose a time

step $\Delta t > 0$ and define the time sequence as $t_n = n\Delta t$ for $n = 0, 1, \ldots$. Then in each time interval $[t_n, t_{n+1}]$, the gradient flow with discrete normalization (GFDN) is given by

$$\begin{aligned}
\partial_t \phi_1(\mathbf{x}, t) &= -\Big(H + \beta_s(|\phi_1|^2 + |\phi_0|^2 - |\phi_{-1}|^2)\Big)\,\phi_1 - \beta_s\,\phi_0^2\phi_{-1}^* - B\phi_0, \\
\partial_t \phi_0(\mathbf{x}, t) &= -\Big(H + \beta_s(|\phi_1|^2 + |\phi_{-1}|^2)\Big)\,\phi_0 - 2\beta_s\,\phi_1\phi_0^*\phi_{-1} - B^*\phi_1 - B\phi_{-1}, \qquad (2.5) \quad \{DNGL\} \\
\partial_t \phi_{-1}(\mathbf{x}, t) &= -\Big(H + \beta_s(|\phi_{-1}|^2 + |\phi_0|^2 - |\phi_1|^2)\Big)\,\phi_{-1} - \beta_s\,\phi_1^*\phi_0^2 - B^*\phi_0,
\end{aligned}$$

followed by a projection step as

$$\phi_j(\mathbf{x}, t_{n+1}^+) := \frac{\phi_j(\mathbf{x}, t_{n+1}^-)}{\|\Phi(\cdot, t_{n+1}^-)\|}, \qquad j = 1, 0, -1, \qquad (2.6) \quad \{Projection\}$$

where $\phi_j(\mathbf{x}, t_{n+1}^{\pm}) = \lim_{t \to t_{n+1}^{\pm}} \phi_j(\mathbf{x}, t)$ $(j = 1, 0, -1)$. The gradient flow in (2.5)–(2.6) can be viewed as first applying the steepest descent method to the energy functional in (1.4) without constraint and then projecting the solution back to the unit sphere to satisfy the normalization constraint in (2.3).

In order to solve (2.5)–(2.6) numerically, we discretize (2.5) by using the sine pseudo-spectral method for spatial derivatives and the backward/forward Euler scheme for linear/nonlinear terms for temporal derivatives [3, 31]. Then at the end of each time step, the normalization is achieved by the projection described in (2.6). In the following, we will give a detailed description of our numerical method. Notice that because of the confinement of the trapping potential, the wave function Φ in (2.5) decays to zero exponentially fast when $|\mathbf{x}| \to \infty$. Thus, in practical computations, we can truncate the problem into a bounded computational domain Ω with homogeneous Dirichlet boundary conditions, i.e.,

$$\phi_j(\mathbf{x}, t)|_{\partial\Omega} = 0, \quad t \geq 0, \qquad j = 1, 0, -1. \qquad (2.7) \quad \{\}$$

For simplicity of notations, next we will introduce the scheme for the one-dimensional (1D) GFDN in a bounded domain $\Omega = [a, b]$. Generalizations to higher dimensions are straightforward for tensor product grids. For an integer $K > 0$, define the spatial mesh size $\Delta x = (b - a)/K > 0$ and denote grid points $x_k = a + k\Delta x$ for $k = 0, 1, \ldots, K$. Let $\phi_{j,k}^n$ be the approximation of $\phi_j(x_k, t_n)$ and Φ_j^n be a vector consisting of $\phi_{j,k}^n$ for the j-th component. Denote Φ^n a vector with sub-vectors Φ_j^n for $j = 1, 0, -1$. Then over each interval $[t_n, t_{n+1}]$, the GFDN in (2.5) is discretized as

$$\frac{\phi_{j,k}^\dagger - \phi_{j,k}^n}{\Delta t} = \frac{1}{2} D_{xx}^s \phi_{j,k}^\dagger|_{x=x_k} - \alpha_j^n \left(\phi_{j,k}^\dagger - \phi_{j,k}^n\right) + P_{j,k}^n, \quad 1 \leq k \leq K - 1, \qquad (2.8) \quad \{scheme1\}$$

for $j = 1, 0, -1$, and the projection step in (2.6) is discretized as

$$\phi_{j,k}^{n+1} = \frac{\phi_{j,k}^\dagger}{\|\Phi^\dagger\|} \qquad \text{with} \qquad \|\Phi^\dagger\| = \sqrt{\Delta x \sum_{j=-1}^{1} \sum_{k=1}^{K-1} |\phi_{j,k}^\dagger|^2}\,, \qquad (2.9) \quad \{\}$$

where $P_{j,k}^n$ $(j = 1, 0, -1)$ are defined by

$$P_{1,k}^n := -\Big(V_1(x_k) + \beta_n \sum_{j=-1}^{1} |\phi_{j,k}^n|^2 + \beta_s(|\phi_{1,k}^n|^2 + |\phi_{0,k}^n|^2 - |\phi_{-1,k}^n|^2)\Big)\phi_{1,k}^n$$

$$
\begin{aligned}
& -\beta_s(\phi^n_{0,k})^2(\phi^n_{-1,k})^* - B(x_k)\phi^n_{0,k}, \\
P^n_{0,k} &:= -\Big(V_1(x_k) + \beta_n \sum_{j=-1}^{1} |\phi^n_{j,k}|^2 + \beta_s(|\phi^n_{1,k}|^2 + |\phi^n_{-1,k}|^2)\Big)\phi^n_{0,k} \\
& -2\beta_s\phi^n_{1,k}(\phi^n_{0,k})^*\phi^n_{-1,k} - B^*(x_k)\phi^n_{1,k} - B(x_k)\phi^n_{-1,k}, \\
P^n_{-1,k} &:= -\Big(V_1(x_k) + \beta_n \sum_{j=-1}^{1} |\phi^n_{j,k}|^2 + \beta_s(|\phi^n_{-1,k}|^2 + |\phi^n_{0,k}|^2 - |\phi^n_{1,k}|^2)\Big)\phi^n_{-1,k} \\
& -\beta_s(\phi^n_{0,k})^2(\phi^n_{1,k})^* - B^*(x_k)\phi^n_{0,k}.
\end{aligned}
$$

In (2.8), D^s_{xx} is a pseudo-spectral differential operator approximating ∂_{xx}, which is defined by

$$
D^s_{xx}U|_{x=x_k} = \sum_{l=1}^{K-1} \left(-\mu_l^2 \widehat{U}_l\right) \sin\left(\mu_l(x_k - a)\right), \qquad 1 \le k \le K-1, \tag{2.10}
$$

{*operator*}

where $\widehat{U}_l$ denotes the l-th coefficient of the sine transform of the vector $U = (U_1, U_2, \ldots, U_{K-1})^T$, i.e.,

$$
\widehat{U}_l = \frac{2}{K} \sum_{k=1}^{K-1} U_k \sin\left(\mu_l(x_k - a)\right) \qquad \text{and} \qquad \mu_l = \frac{l\pi}{b-a}, \qquad 1 \le l \le K-1.
$$

The constant $\alpha^n_j \ge 0$ $(j = 1, 0, -1)$ is the stabilization parameter, which is chosen in the "optimal" form (such as the time step can be chosen as large as possible) (see, e.g. [31, 6, 17]). The initial condition is discretized as

$$
\phi^0_{j,k} = \phi_j(x_k, 0), \qquad 0 \le k \le K, \quad j = 1, 0, -1, \tag{2.11}
$$

{*dinitial*}

and the boundary conditions are

$$
\phi^n_{j,0} = \phi^n_{j,K} = 0, \qquad n = 0, 1, \ldots, \quad j = 1, 0, -1. \tag{2.12}
$$

{*dbc*}

The discrete system (2.8), (2.11) and (2.12) can be efficiently solved by the sine transform. In fact, taking the sine transform at both sides of (2.8), we get

$$
\frac{\widehat{\phi}^{\dagger}_{j,l} - \widehat{\phi}^n_{j,l}}{\Delta t} = -\frac{1}{2}\mu_l^2\, \widehat{\phi}^{\dagger}_{j,l} - \alpha^n_j \left(\widehat{\phi}^{\dagger}_{j,l} - \widehat{\phi}^n_{j,l}\right) + \widehat{P}^n_{j,l}, \qquad l = 1, 2, \ldots, K-1, \tag{2.13}
$$

{}

which implies that

$$
\widehat{\phi}^{\dagger}_{j,l} = \frac{\left(1 + \alpha^n_j \Delta t\right)\widehat{\phi}^n_{j,l} + \widehat{P}^n_{j,l}}{1 + \left(\alpha^n_j + \mu_l^2/2\right)\Delta t}, \qquad j = 1, 0, -1 \tag{2.14}
$$

{}

for $l = 1, 2, \ldots, K-1$ and $n = 0, 1, \ldots$. Since the sine transform is used, the memory required to solve the above system is $O(K)$ and computational cost per time step is $O(K \ln(K))$. The simulation is stopped by requiring that

$$
\max_{-1 \le j \le 1} \max_{1 \le k \le K-1} \frac{|\phi^{n+1}_{j,k} - \phi^n_{j,k}|}{\Delta t} < \varepsilon, \tag{2.15}
$$

{}

where ε is a chosen tolerance. The resulting solution $\Phi := \lim_{n\to\infty} \Phi^{n+1}$ is the ground state of the spin-1 BECs.

3 Numerical methods for ground states with $B = 0$

{*section3*}

In Section 2, we present a numerical method to compute the ground states of spin-1 BECs when $B(\mathbf{x}) \neq 0$, while in this section we will consider the case with $B(\mathbf{x}) \equiv 0$. In the former case, the ground state is defined as the minimizer of the energy under the constraints of normalization. However, when $B(\mathbf{x}) \equiv 0$, they also need to satisfy the conservation of magnetization defined in (1.6). In detail, the ground state $\Phi_{0,g}(\mathbf{x})$ in this case is defined by

Find ($\Phi_{0,g} \in S_0$) such that

$$E_{0,g} := E_0(\Phi_{0,g}) = \min_{\Phi \in S_0} E_0(\Phi), \tag{3.1}$$ {*minimizer1*}

where E_0 is the energy functional defined in (1.5) and S_0 is a nonconvex set defined by

$$S_0 := \left\{ \Phi = (\phi_1,\, \phi_0,\, \phi_{-1})^T \;\mid\; \|\Phi(\cdot)\|^2 = 1, \quad \|\phi_1(\cdot)\|^2 - \|\phi_{-1}(\cdot)\|^2 = M, \quad E_0(\Phi) < \infty \right\},$$

with $-1 \leq M \leq 1$ a given fixed total magnetization. In the case of $B(\mathbf{x}) \equiv 0$, when $\beta_n > 0$, $|\beta_s| \leq \beta_n$ and $\lim_{|\mathbf{x}|\to\infty} V_d(\mathbf{x}) = \infty$, the existence of a minimizer of the nonconvex minimization problem (3.1) follows from the standard theory [8]. In fact, $E_0(\alpha \cdot \Phi_{0,g}) = E_0(\Phi_{0,g})$ for all constant vector $\alpha = (e^{i\theta_1}, e^{i\theta_0}, e^{i\theta_{-1}})^T$ with $\theta_1 + \theta_{-1} - 2\theta_0 = 2m\pi$ for any integer m. Thus, the uniqueness is up to gauge transform [28] and was studied in [18].

Similarly, the ground state $\Phi_{0,g}(\mathbf{x})$ can also be considered as the eigenfunctions of the following Euler-Lagrange equations:

$$\begin{aligned}
(\mu+\lambda)\phi_1 &= \left(H + \beta_s(|\phi_1|^2 + |\phi_0|^2 - |\phi_{-1}|^2)\right)\phi_1 + \beta_s\,\phi_0^2\phi_{-1}^*, \\
\mu\phi_0 &= \left(H + \beta_s(|\phi_1|^2 + |\phi_{-1}|^2)\right)\phi_0 + 2\beta_s\,\phi_1\phi_0^*\phi_{-1}, \\
(\mu-\lambda)\phi_{-1} &= \left(H + \beta_s(|\phi_{-1}|^2 + |\phi_0|^2 - |\phi_1|^2)\right)\phi_{-1} + \beta_s\,\phi_1^*\phi_0^2,
\end{aligned} \tag{3.2}$$ {*SGPEs*}

under the constraints

$$\|\Phi(\cdot)\|^2 := \sum_{j=-1}^{1} \int_{\mathbb{R}^d} |\phi_j(\mathbf{x})|^2 d\mathbf{x} = 1, \qquad \int_{\mathbb{R}^d} \left(|\phi_1(\mathbf{x})|^2 - |\phi_{-1}(\mathbf{x})|^2\right) d\mathbf{x} = M, \tag{3.3}$$ {*constraint1*}

where μ and λ are the Lagrange multipliers (or chemical potentials) of the coupled time-independent GPEs (3.2)–(3.3). The GPEs in (3.2) can be also obtained from its time-dependent counterpart (1.1) with $B(\mathbf{x}) \equiv 0$ by substituting the ansatz

$$\psi_{\pm1}(\mathbf{x}, t) = e^{-i(\mu\pm\lambda)t}\phi_{\pm1}(\mathbf{x}), \qquad \psi_0(\mathbf{x}, t) = e^{-i\mu t}\phi_0(\mathbf{x}). \tag{3.4}$$ {*ansatz*}

Recently, there have been numerical methods proposed in the literature (see, e.g., [5, 6, 17, 9]) to compute the ground states of spin-1 BECs when $B(\mathbf{x}) = 0$, in which the system of three-component equations was solved. However, we notice that when $B(\mathbf{x}) = 0$, the ground states of spin-1 BECs in fact can be described by a single-mode or two-component reduction based on their ferromagnetic or antiferromagnetic characterizations [18]. As a result, we can introduce numerical methods based on the characterization of spin-1 BECs so as to reduce the computational costs of the methods given in the literature. In the following, we will discuss the ferromagnetic and antiferromagnetic system separately, and for each system, we will start with reviewing its characterization properties and then propose numerical methods for the reduced system.

3.1 Ferromagnetic system

{*section3-1*}

Experimental observations [15, 24, 13] and numerical simulations [30, 5, 6, 17] suggest that in ferromagnetic ($\beta_s < 0$) spin-1 BECs, each component of the ground state is a multiple of one single density function. This is so-called the *single-mode approximation (SMA)* in the literature, which has been justified rigorously in mathematics by Lin and Chern in [18]. In this case, one can compute just one density function instead of three. To do this, we denote $\rho(\mathbf{x}) \geq 0$, for $\mathbf{x} \in \mathbb{R}^d$, as a scalar real-valued density function and require it satisfy the normalization condition

$$\|\rho(\cdot)\|^2 = \int_{\mathbb{R}^d} \rho^2(\mathbf{x})\, d\mathbf{x} = 1. \tag{3.5}$$ {*normal-rho*}

Let[1] $\Phi_g(\mathbf{x}) = (\phi_{1,g}, \phi_{0,g}, \phi_{-1,g})^T$ be the ground state of a ferromagnetic spin-1 BEC and according to the single-mode approximation, we can set

$$\phi_{j,g}(\mathbf{x}) = |\phi_{j,g}(\mathbf{x})| = \gamma_j\, \rho(\mathbf{x}), \qquad j = 1,\, 0,\, -1, \tag{3.6}$$ {*SMA*}

with constants $\gamma_j \geq 0$ (for $j = 1, 0, -1$). Noticing that the ground state $\Phi_g(\mathbf{x})$ is defined under the constraints of normalization and magnetization given in (3.3), we obtain

$$\gamma_1^2 + \gamma_0^2 + \gamma_{-1}^2 = 1, \qquad \gamma_1^2 - \gamma_{-1}^2 = M. \tag{3.7}$$ {*gamma*}

Substituting (3.6) into (1.5) and taking (3.7) into account, we have

$$\begin{aligned} E_0(\Phi_g) \;=\; & \int_{\mathbb{R}^d} \bigg[\frac{1}{2}|\nabla\rho(\mathbf{x})|^2 + V_d(\mathbf{x})\rho^2(\mathbf{x}) + \frac{\beta_n}{2}\rho^4(\mathbf{x}) \\ & + \frac{\beta_s}{2}\left(M^2 + 2\gamma_0^2(\gamma_1+\gamma_{-1})^2\right)\rho^4(\mathbf{x})\bigg] d\mathbf{x}. \end{aligned} \tag{3.8}$$ {*1componentE*}

Notice that the minimization of (3.8) over ρ and $(\gamma_1, \gamma_0, \gamma_{-1})$ is separable. Thus, we can take minimization of (3.8) first over $(\gamma_1, \gamma_0, \gamma_{-1})$ and then over ρ. Furthermore, since $\beta_s < 0$, we should consider

$$\max_{\gamma_1,\gamma_0,\gamma_{-1}} \left\{M^2 + 2\gamma_0^2(\gamma_1+\gamma_{-1})^2\right\}, \qquad \text{subject to} \quad (3.7),$$

which gives the constants

$$\gamma_0 = \sqrt{\frac{1}{2}\,(1-M^2)}, \qquad \gamma_{\pm 1} = \frac{1}{2}\,(1 \pm M)\,. \tag{3.9}$$ {*coefficient*}

Taking (3.9) into account, we define the SMA energy

$$E_{\rm sma}(\rho) \;=\; \int_{\mathbb{R}^d} \bigg[\frac{1}{2}|\nabla\rho(\mathbf{x})|^2 + V_d(\mathbf{x})\rho^2(\mathbf{x}) + \frac{\kappa}{2}\rho^4(\mathbf{x})\bigg] d\mathbf{x} \tag{3.10}$$ {*SMAE*}

with the constant $\kappa = \beta_n + \beta_s$. It is obvious that the function ρ in (3.6) should minimize the SMA energy in (3.10) with the constraint (3.5) [18].

[1]For simplicity of notation, in the following sections we will also use $\Phi_g(\mathbf{x})$ to represent the ground state of the condensate with $B(\mathbf{x}) \equiv 0$. To distinguish it from those when $B(\mathbf{x}) \neq 0$, one should refer to the context of the discussion.

We see that for a ferromagnetic system, one can first solve for the density function ρ which minimizes the SMA energy $E_{\rm sma}$ subject to the normalization constraint in (3.5), and then obtain the ground state of the corresponding spin-1 BECs by considering (3.6) and (3.9). In detail, we solve the following single-component minimization problem:

Find $(u_g(\mathbf{x}) \in S_{\rm sma})$ such that

$$E_{{\rm sma},g} := E_{\rm sma}(u_g) = \min_{u\in S_{\rm sma}} E_{\rm sma}(u) \tag{3.11}$$ {*minimizer-SMA*}

over the set

$$S_{\rm sma} = \left\{ u(\mathbf{x}) \in \mathbb{R} \mid \int_{\mathbb{R}^d} u^2\, d\mathbf{x} = 1, \quad E_{\rm sma}(u) < \infty \right\}.$$

Then the density $\rho(\mathbf{x})$ in (3.6) is given by $u_g(\mathbf{x})$, i.e., $\rho(\mathbf{x}) \equiv u_g(\mathbf{x})$. The Euler-Lagrange equation corresponding to (3.11) is given by

$$\mu_{\rm sma}\, u(\mathbf{x}) = -\frac{1}{2}\nabla^2 u(\mathbf{x}) + V_d(\mathbf{x})u(\mathbf{x}) + \kappa u^3(\mathbf{x}), \tag{3.12}$$ {*1componentGPE*}

with the constraint $\|u(\cdot)\|^2 = 1$. This is a nonlinear eigenvalue problem with the normalization constraint and the eigenvalue $\mu_{\rm sma}$ can be computed by

$$\mu_{\rm sma}(u) \quad = \quad \int_{\mathbb{R}^d} \left[\frac{1}{2}|\nabla u(\mathbf{x})|^2 + V_d(\mathbf{x})u^2(\mathbf{x}) + \kappa u^4(\mathbf{x}) \right] d\mathbf{x}. \tag{3.13}$$ {}

Similar to that in Section 2, our numerical scheme will be introduced based on the gradient flow with discrete normalization and its discretization will be presented for 1D case for simplicity. Generalizations of the method to higher dimensions are straightforward. For $t \in [t_n, t_{n+1}]$, the 1D GFDN corresponding to (3.11) is given by

$$\partial_t u(x,t) = \frac{1}{2}\nabla^2 u - V_1(x)u - \kappa u^3, \qquad x \in [a,b], \quad t \in [t_n, t_{n+1}], \tag{3.14}$$ {*DNGF*}

$$u(x, t_{n+1}^+) := \frac{u(x, t_{n+1}^-)}{\|u(\cdot, t_{n+1}^-)\|}, \qquad x \in [a,b], \tag{3.15}$$ {*projection*}

where the computational domain is truncated into a sufficiently large interval $[a,b]$ and homogeneous Dirichlet boundary conditions $u(a,t) = u(b,t) = 0$ are imposed. At time $t = 0$, the initial condition is given by

$$u(x,0) = u_0(x), \quad x \in [a,b] \qquad \text{with} \quad \|u_0(\cdot)\| = 1. \tag{3.16}$$ {*initial-single*}

To discretize the gradient flow (3.14)–(3.16), we use the sine pseudo-spectral method for spatial derivatives and the backward/forward Euler scheme for linear/nonlinear terms for the time derivative. The scheme is given as below:

$$\frac{u_k^\dagger - u_k^n}{\Delta t} = \frac{1}{2} D_{xx}^s u^\dagger|_{x=x_k} - \alpha^n (u_k^\dagger - u_k^n) + F_k^n, \quad k = 1, 2, \ldots, K-1, \tag{3.17}$$ {*scheme*}

$$u_k^{n+1} = \frac{u_k^\dagger}{\|\mathbf{u}^\dagger\|}, \qquad k = 1, 2, \ldots, K-1, \quad n = 0, 1, \ldots. \tag{3.18}$$ {}

where $\|\mathbf{u}^\dagger\| = \sqrt{\Delta x \sum_{k=1}^{K-1} (u_k^\dagger)^2}$, and

$$F_k^n := F(u_k^n) = -\left(V_1(x_k)u_k^n + \kappa(u_k^n)^3\right), \qquad k = 1, 2, \ldots, K-1. \tag{3.19}$$ {}

The operator D_{xx}^s is defined as in (2.10). The stabilization parameter $\alpha^n \geq 0$ is chosen as [31, 4]

$$\alpha^n = \frac{1}{2}\left[\max_{1\leq k\leq K-1}\left(V_1(x_k) + \kappa(u_k^n)^2\right) + \min_{1\leq k\leq K-1}\left(V_1(x_k) + \kappa(u_k^n)^2\right)\right].$$

The initial and boundary conditions are discretized as

$$u_k^0 = u_0(x_k), \quad k = 0, 1, \ldots, K; \qquad u_0^n = u_K^n = 0, \quad n = 0, 1, \ldots, \tag{3.20}$$ {}

respectively. This discrete system can be efficiently solved in the same manner as that for (2.8), (2.11) and (2.12).

3.2 Antiferromagnetic system

{*section3-2*}

In an antiferromagnetic ($\beta_s > 0$) system, the density distribution of atoms in ground states highly depends on the total magnetization M. It was shown in [18] that if $M \neq 0$, the ground states have vanishing zeroth $m_F = 0$ component, i.e., $\phi_{0,g}(\mathbf{x}) \equiv 0$. As a result, the original three-component system is indeed characterized by a two-component reduction. However, if $M = 0$, the ground states of three components have the same density distribution so that they can be described by the SMA as given in (3.6). But different from ferromagnetic systems, in this case the constants γ_j are not unique and they are given by $\gamma_1 = \gamma_{-1} = \xi$ and $\gamma_0 = \sqrt{1-2\xi^2}$ for any constant $\xi \in [0, 1/\sqrt{2}]$. For the detailed mathematical proof, we refer the readers to [18]. In the following, we review the two-component reduction and discretize it for computing the ground state of antiferromagnetic spin-1 BECs when $M \neq 0$. For the case of $M = 0$, the numerical method is identical to that we described in Section 3.1 and thus it is omitted here for brevity.

Let $\Phi_g(\mathbf{x})$ be the ground state of an antiferromagnetic spin-1 BEC with $M \neq 0$. Since $\phi_{0,g}(\mathbf{x}) \equiv 0$, the ground state energy $E_{0,g}$ reduces to

$$\begin{aligned} E_0(\Phi_g) = \int_{\mathbb{R}^d} \Big[&\frac{1}{2}\left(|\nabla\phi_{1,g}|^2 + |\nabla\phi_{-1,g}|^2\right) + V_d(\mathbf{x})\left(|\phi_{1,g}|^2 + |\phi_{-1,g}|^2\right) \\ &+ \frac{\chi}{2}\left(|\phi_{1,g}|^4 + |\phi_{-1,g}|^4\right) + \nu|\phi_{1,g}|^2|\phi_{-1,g}|^2\Big] d\mathbf{x}, \end{aligned} \tag{3.21}$$ {}

where the constants $\chi = \beta_n + \beta_s$ and $\nu = \beta_n - \beta_s$. From the constraints of normalization and magnetization in (3.3), it is easy to obtain

$$\int_{\mathbb{R}^d} |\phi_{1,g}(\mathbf{x})|^2 d\mathbf{x} = \frac{1+M}{2}, \qquad \int_{\mathbb{R}^d} |\phi_{-1,g}(\mathbf{x})|^2 d\mathbf{x} = \frac{1-M}{2}. \tag{3.22}$$ {*constraints-TMA*}

On the other hand, we define a two-component energy

$$E_{\rm tca}(u_1, u_2) := \int_{\mathbb{R}^d} \left[\sum_{j=1}^{2}\left(\frac{1}{2}|\nabla u_j|^2 + V_d(\mathbf{x})|u_j|^2\right) + \frac{\chi}{2}\left(|u_1|^4 + |u_2|^4\right) + \nu|u_1|^2|u_2|^2\right] d\mathbf{x}. \tag{3.23}$$ {}

It is easy to verify that the ground state $(\phi_{1,g}, \phi_{-1,g})$ minimizes the energy $E_{\rm tca}$ under the constraints (3.22). Hence, the minimization problem defined in (3.1) to find the ground state of an antiferromagnetic spin-1 condensate can be reduced to the following two-component minimization problem:

Find $((u_{1,g}, u_{2,g}) \in S_{\rm tca})$, such that

$$E_{{\rm tca},g} := E_{\rm tca}(u_{1,g}, u_{2,g}) = \min_{(u_1,u_2)\in S_{\rm tca}} E_{\rm tca}(u_1, u_2) \tag{3.24}$$ {*minimizer5*}

over the set

$$S_{\rm tca} = \Big\{(u_1, u_2) \mid \|u_1\|^2 = (1+M)/2, \quad \|u_2\|^2 = (1-M)/2, \quad E_{\rm tca}(u_1, u_2) < \infty\Big\}.$$

The ground state of the associated antiferromagnetic spin-1 BECs can be obtained by

$$\phi_{1,g}(\mathbf{x}) = u_{1,g}(\mathbf{x}), \qquad \phi_{0,g}(\mathbf{x}) \equiv 0, \qquad \phi_{-1,g}(\mathbf{x}) = u_{2,g}(\mathbf{x}). \tag{3.25}$$ {}

The Euler-Lagrange equations corresponding to the minimization problem in (3.24) are given by

$$\begin{aligned} \mu_1^{\rm tca}\, u_1(\mathbf{x}) &= \left(-\frac{1}{2}\nabla^2 + V_d(\mathbf{x}) + \chi|u_1(\mathbf{x})|^2 + \nu|u_2(\mathbf{x})|^2\right) u_1(\mathbf{x}), \\ \mu_2^{\rm tca}\, u_2(\mathbf{x}) &= \left(-\frac{1}{2}\nabla^2 + V_d(\mathbf{x}) + \nu|u_1(\mathbf{x})|^2 + \chi|u_2(\mathbf{x})|^2\right) u_2(\mathbf{x}), \end{aligned} \tag{3.26}$$ {*2componentGPE*}

with the constrains $\|u_1\|^2 = (1+M)/2$ and $\|u_2\|^2 = (1-M)/2$, where the two-component chemical potentials are defined by

$$\mu_j^{\rm tca} = \int_{\mathbb{R}^d} \left[\frac{1}{2}|\nabla u_j|^2 + V_d(\mathbf{x})|u_j|^2 + \chi|u_j|^4 + \nu|u_j|^2|u_{l\neq j}|^2\right] d\mathbf{x}, \quad j, l = 1, 2. \tag{3.27}$$ {}

To find the ground states defined in (3.24), a gradient flow with discrete normalization for two-component system is used over each time interval $[t_n, t_{n+1}]$ for $n = 0, 1, \ldots$, i.e.,

$$\partial_t u_j(\mathbf{x}, t) = \left(\frac{1}{2}\nabla^2 - V_d(\mathbf{x}) - \chi|u_j|^2 - \nu|u_{l\neq j}|^2\right) u_j(\mathbf{x}, t), \qquad j, l = 1, 2, \tag{3.28}$$ {*BMA1*}

$$u_1(\mathbf{x}, t_{n+1}) = \sqrt{\frac{1+M}{2}}\, \frac{u_1(\mathbf{x}, t_{n+1}^-)}{\|u_1(\cdot, t_{n+1}^-)\|}, \quad u_2(\mathbf{x}, t_{n+1}) = \sqrt{\frac{1-M}{2}}\, \frac{u_2(\mathbf{x}, t_{n+1}^-)}{\|u_2(\cdot, t_{n+1}^-)\|}, \tag{3.29}$$ {*BMA3*}

and at time $t = 0$, the initial conditions are given by

$$u_j(\mathbf{x}, 0) = u_{j,0}(\mathbf{x}), \quad j = 1, 2 \quad \text{with} \quad \|u_{1,0}(\cdot)\| = \sqrt{\frac{1+M}{2}}, \quad \|u_{2,0}(\cdot)\| = \sqrt{\frac{1-M}{2}}. \tag{3.30}$$ {*initial1*}

In practical computations, the above gradient flow can be solved in a bounded domain Ω with the homogeneous Dirichlet boundary conditions

$$u_1(\mathbf{x}, t) = u_2(\mathbf{x}, t) = 0, \qquad \mathbf{x} \in \partial\Omega, \quad t \geq 0, \tag{3.31}$$ {*BC*}

due to the confinement of the external potential.

Next we will give the discretization of (3.28)–(3.31) in the 1D case with $\Omega = [a, b]$. Let $u_{j,k}^n$ be the numerical approximation of $u_j(x_k, t_n)$ for $j = 1, 2$. Then we have

$$\frac{u_{j,k}^\dagger - u_{j,k}^n}{\Delta t} = \frac{1}{2} D_{xx}^s \, u_j^\dagger|_{x=x_k} - \alpha_j^n (u_{j,k}^\dagger - u_{j,k}^n) + G_{j,k}^n, \qquad j = 1, 2, \tag{3.32}$$ {discretization2}

$$u_{1,k}^{n+1} = \sqrt{\frac{1+M}{2}} \frac{u_{1,k}^\dagger}{\|\mathbf{u}_1^\dagger\|}, \quad u_{2,k}^{n+1} = \sqrt{\frac{1-M}{2}} \frac{u_{2,k}^\dagger}{\|\mathbf{u}_2^\dagger\|}, \qquad 1 \le k \le K-1, \tag{3.33}$$ {}

where $\|\mathbf{u}_j^\dagger\| = \sqrt{\Delta x \sum_{k=1}^{K-1} |u_{j,k}^\dagger|^2}$ for $j = 1, 2$, and

$$G_{j,k}^n = -\left(V_1(x_k) + \chi |u_{j,k}^n|^2 + \nu |u_{l\neq j,k}^n|^2\right) u_{j,k}^n, \qquad 1 \le k \le K-1$$

for $j, l = 1, 2$, and the stabilization parameters α_j^n $(j = 1, 2)$ are chosen as

$$\alpha_j^n = \frac{1}{2}\left[\max_k \left(V_1(x_k) + \chi |u_{j,k}^n|^2 + \nu |u_{l\neq j,k}^n|^2\right) + \min_k \left(V_1(x_k) + \chi |u_{j,k}^n|^2 + \nu |u_{l\neq j,k}^n|^2\right)\right].$$

The operator D_{xx}^s is defined in (2.10). The homogeneous Dirichlet boundary conditions are discretized as

$$u_{1,0}^{n+1} = u_{1,K}^{n+1} = u_{2,0}^{n+1} = u_{2,K}^{n+1} = 0, \qquad n = 0, 1, \ldots, \tag{3.34}$$ {}

and the initial conditions are discretized as

$$u_{1,k}^0 = u_1^0(x_k), \quad u_{2,k}^0 = u_2^0(x_k), \qquad k = 0, 1, \ldots, K. \tag{3.35}$$ {initial2}

For each time step, the discrete system (3.32)–(3.35) can be solved in the same manner as that for (2.8), (2.11) and (2.12).

3.3 Relation between different minimization problems

{section3-3}

As we have seen, the ground states of spin-1 BECs are always defined by constrained minimization problems, e.g., (2.1) for $B \neq 0$ and (3.1) for $B \equiv 0$. In the following, we will describe the relation between different minimization problems.

When $B = 0$, the ground state can be obtained by minimizing the energy functional E_0 subject to the conservation of both normalization and magnetization. While $B \neq 0$, the energy E is minimized by requiring only the conservation of normalization. To see the relation between these two minimization problems, we can introduce Φ_g^M defined by

Find $(\Phi_g^M \in S^M)$, such that

$$E_g^M := E(\Phi_g^M) = \min_{\Phi \in S^M} E(\Phi), \tag{3.36}$$ {minimizer9}

where for a given $M \in [-1, 1]$, the set S^M is defined as

$$S^M := \left\{\Phi = (\phi_1, \phi_0, \phi_{-1})^T \mid \|\Phi(\cdot)\|^2 = 1, \;\; \|\phi_1(\cdot)\|^2 - \|\phi_{-1}(\cdot)\|^2 = M, \;\; E(\Phi) < \infty\right\}.$$

That is, Φ_g^M is a minimizer of the energy functional E subject to the conservation of both normalization and magnetization M. To obtain the minimizer of the energy E with only

the constraint of normalization, one needs to further minimizer E_g^M in (3.36) with respect to $-1 \le M \le 1$. Thus, the minimization problem in (2.1) is equivalent to

Find $(\Phi_g \in S)$, such that

$$E(\Phi_g) = \min_{M\in[-1,1]} E(\Phi_g^M) = \min_{M\in[-1,1]} \min_{\Phi\in S^M} E(\Phi), \tag{3.37}$$ {*minimizer8*}

which decomposes (2.1) into two minimization problems. The inner minimization problem is similar to that defined in (3.1) but with different energy functional, while the outer minimization only involves one variable $M \in [-1, 1]$. In the form of (3.37), one can see the effect of the magnetization M on the ground states when $B \neq 0$.

On the other hand, the minimization problem in (3.1) is over three wave functions ϕ_j (for $j = 1, 0, -1$) subject to two constraints. These constraints specify the normalization and total magnetization of the ground states. However, to better understand each component in the ground state, we want to know the norm of individual component. To this end, we define $\Phi_{0,g}^\alpha(\mathbf{x})$ as the minimizer of the following nonconvex minimization problem:

Find $(\Phi_{0,g}^\alpha \in S_0^\alpha)$, such that

$$E_{0,g}^\alpha := E_0(\Phi_{0,g}^\alpha) = \min_{\Phi\in S_0^\alpha} E_0(\Phi), \tag{3.38}$$ {*minimizer2*}

where $\alpha \in [0, 1]$ is a given constant and S_0^α is a nonconvex set defined as

$$S_0^\alpha := \left\{ \Phi = (\phi_1,\, \phi_0,\, \phi_{-1})^T \mid \|\phi_0(\cdot)\|^2 = \alpha, \quad \|\phi_{\pm1}(\cdot)\|^2 = \frac{1-\alpha \pm M}{2}, \quad E_0(\Phi) < \infty \right\}.$$

The minimization problem (3.38) has three unknowns ϕ_j^α $(j = 1, 0, -1)$ and the same number of constraints, which is much easier than the problem in (3.1). In fact, the minimizer $\Phi_{0,g}^\alpha$ can be viewed as a ground state which satisfies the conservation of the total normalization and magnetization as described in (3.3) and also the conservation of the norm for each component.

It is easy to see that to find the ground states $\Phi_{0,g}$ in (3.1), one can first fix α and obtain $\Phi_{0,g}^\alpha$ by minimizing (3.38), and then minimize $E_{0,g}^\alpha$ over $\alpha \in [0, 1]$. Thus, the problem in (3.1) can be decomposed into two minimizing processes, i.e.,

Find $(\Phi_{0,g} \in S_0)$, such that

$$E_0(\Phi_{0,g}) = \min_{\alpha\in[0,1]} E_0(\Phi_{0,g}^\alpha) = \min_{\alpha\in[0,1]} \min_{\Phi\in S_0^\alpha} E_0(\Phi). \tag{3.39}$$ {*minimizer3*}

By minimizing $E_{0,g}^\alpha$ over $0 \le \alpha \le 1$, one can easily obtain the relation between three components in the ground states.

4 Numerical results

{*section4*}

In this section, we apply our numerical methods to compute the ground states of spin-1 condensates. First, the ground states in the cases of $B(\mathbf{x}) \neq 0$ are studied and some conjectures are made from our numerical observations. In the case of $B(\mathbf{x}) \equiv 0$, we first

compare the performance of our methods with those proposed in the literature [5, 6, 17]. Then we apply our efficient methods to study the ground states of the ferromagnetic and antiferromagnetic spin-1 BECs. In all simulations, the ground states are obtained by setting the tolerance $\varepsilon = 10^{-6}$.

4.1 Numerical results for $B \neq 0$

{*section4-1*}

In this subsection, we study the ground states of spin-1 BECs with $B(\mathbf{x}) \neq 0$. We first start with 1D condensates and both the ferromagnetic and antiferromagnetic systems are considered. Then the ground states of 2D spin-1 BECs are studied with respect to different Ioffe-Pritchard magnetic field B.

Example 1 We study the ground states of 1D spin-1 condensates confined in a harmonic potential $V_1(x) = x^2/2$. The computational domain is $[-32, 32]$; the mesh size and time step are chosen as $\Delta x = 0.03125$ and $\Delta t = 0.001$, respectively. We choose $\beta_n = 400$, and $\beta_s = -250$ and $\beta_s = 250$ for the ferromagnetic and antiferromagnetic cases, respectively. The following two cases are considered:

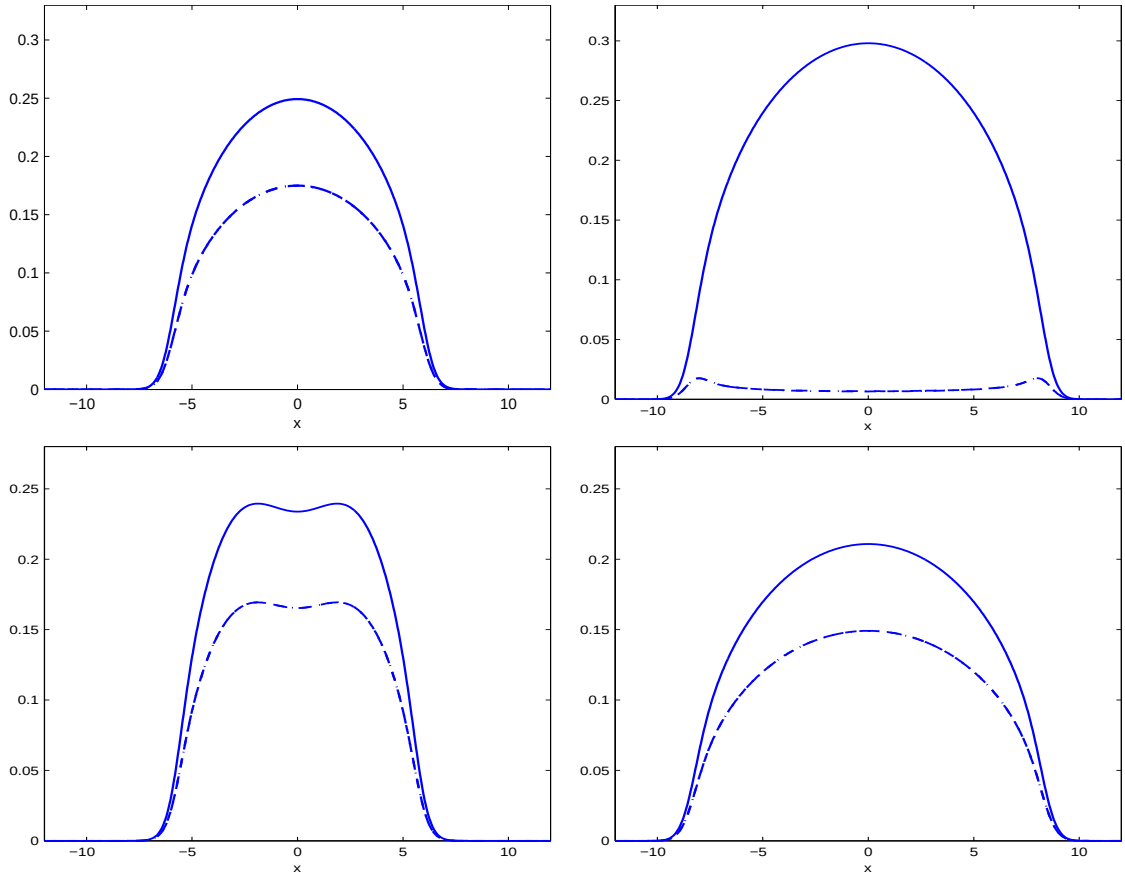

Figure 1: Ground states of spin-1 BECs in Example 1 for ferromagnetic (left) and antiferromagnetic (right) cases with $B(x) = (1+i)\cos x$ (top) and $B(x) = e^{ix}$ (bottom). Dash line: $|\phi_{1,g}|$; solid line: $|\phi_{0,g}|$; dash-dot line: $|\phi_{-1,g}|$. Notice that the graphs of $|\phi_{1,g}|$ and $|\phi_{-1,g}|$ are identical.

{*F1*}

Case I. $B(x) \in \mathbb{C}$ is a periodic function of $x \in \mathbb{R}$. Figure 1 shows the ground states for $B(x) = (1+i)\cos x$ and $B(x) = e^{ix}$. For both ferromagnetic and antiferromagnetic cases, the density function is symmetric with respect to $x = 0$ which is the center of external trap $V_1(x)$. Furthermore, the $m_F = \pm 1$ components of the ground states have the same density, which implies that when $B(x)$ is nonzero, the stationary states with total magnetization $M = 0$ have the lowest energy.

Case II. $B(x) \equiv B \in \mathbb{C}$ is a constant. Figure 2 shows the ground states for the constant $B = 3 + 4i$. From it and our extensive simulations not shown here for brevity, we find that when $B(x)$ is a constant, the ground states satisfy exactly the single-mode approximation defined in (3.6), which is independent of ferromagnetic or antiferromagnetic characterizations. Furthermore, our numerical results suggests that the constants in the SMA (3.6) are given by $\gamma_1 = \gamma_{-1} = \frac{1}{2}$ and $\gamma_0 = \frac{\sqrt{2}}{2}$. In addition, we find that the SMA density function depends only on the interaction parameters β_n and β_s, but not on the constant B. The SMA ground state energy depends on the modules of B, i.e., $|B|$, instead of B.

To further investigate their energy, we study the ground states with respect to different constants β_n, β_s and $|B|$. Figures 3-4 present the ground state energy for ferromagnetic and antiferromagnetic cases, respectively, where in Fig. 4 the real-valued constants B are chosen to illustrate the relation between energy and constant B. From Fig. 3 for ferromagnetic condensates, we see that if the constant $|B|$ is fixed, the larger the constant $\beta_n + \beta_s$, the higher the ground state energy. Furthermore, when $\beta_n + \beta_s$ is large, the energy becomes almost linearly dependent on it. In addition, the energy linearly decreases for a larger $|B|$, if the summation $\beta_n + \beta_s$ is fixed. On the other hand, in antiferromagnetic cases, the energy decreases when a larger $|B|$ is imposed. However, the same constants $\beta_n + \beta_s$ and $|B|$ may result in different ground state energy (see Fig. 4 (right)), which is different from the ferromagnetic cases.

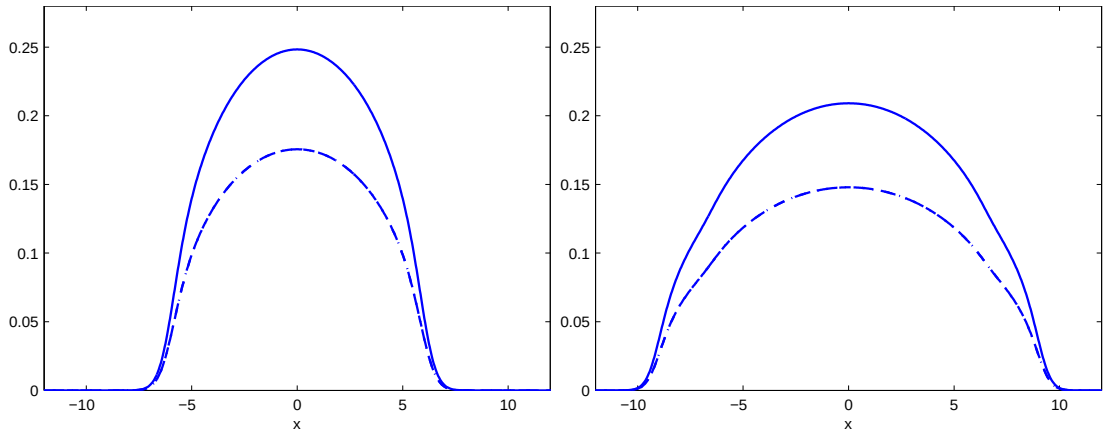

Figure 2: Ground states of spin-1 BECs in Example 1 for ferromagnetic (left) and antiferromagnetic (right) cases with $B(x) \equiv 3 + 4i$, where dash line: $|\phi_{1,g}|$, solid line: $|\phi_{0,g}|$, and dash-dot line: $|\phi_{-1,g}|$. Notice that the graphs of $|\phi_{1,g}|$ and $|\phi_{-1,g}|$ are identical. {F2}

Example 2 We study the ground states of 2D spin-1 BECs in an isotropic harmonic potential $V_2(\mathbf{x}) = (x^2 + y^2)/2$. Figures 5-7 show the density functions of the ground states for $B(x, y) = \sin(x) + \sin(y)$, $\sin(x) + i\sin(y)$ and $1 + 2i$, respectively. Similar to the

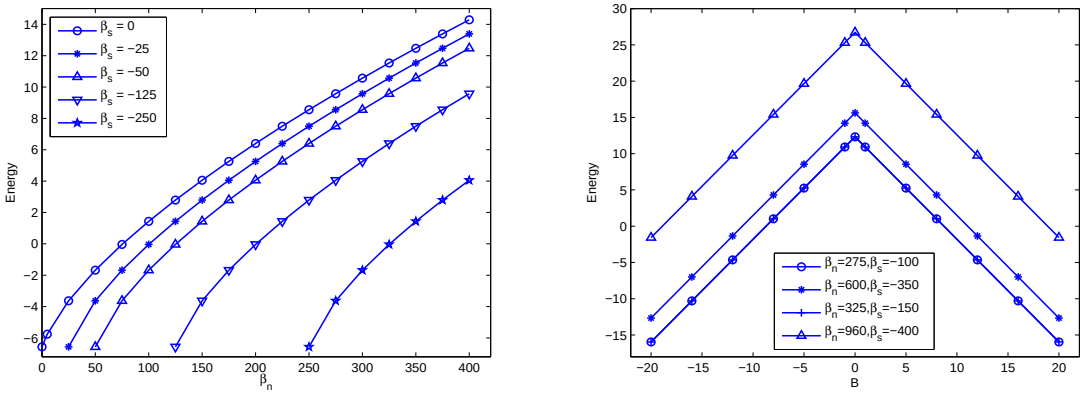

Figure 3: Energy versus the interaction parameter β_n with $|B| = 5$ fixed (left) and versus the constant B (right) in ferromagnetic cases. {F3}

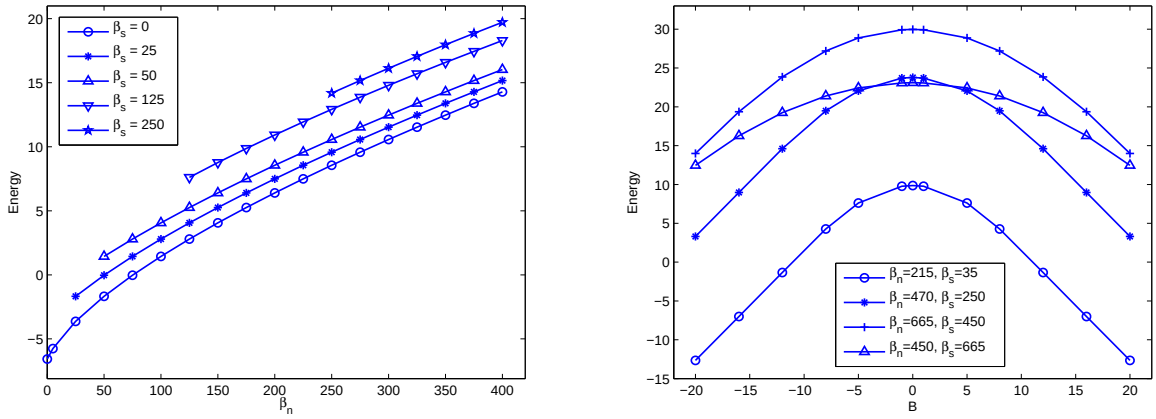

Figure 4: Energy versus the interaction parameter β_n with $|B| = 5$ fixed (left) and versus the constant B (right) in antiferromagnetic cases. {F4}

1D case, the densities of $m_F = \pm 1$ components in the ground states are identical, which is true for both ferromagnetic and antiferromagnetic condensates. Furthermore, if the complex-valued $B(x, y)$ is space-dependent, then vortices appear in the ground states; see Fig. 6. However, if $B(x, y) \equiv B$ is a constant, no vortex is observed. In addition, the ground states in this case satisfy the SMA, and the constants γ_j are always $\gamma_{\pm 1} = \frac{1}{2}$ and $\gamma_0 = \frac{\sqrt{2}}{2}$ for any constant B.

4.2 Numerical results for $B = 0$

In this subsection, we first compare our methods in Section 3 to that in the literature [6]. Then we apply them to study the ground states in the case of $B(\mathbf{x}) = 0$.

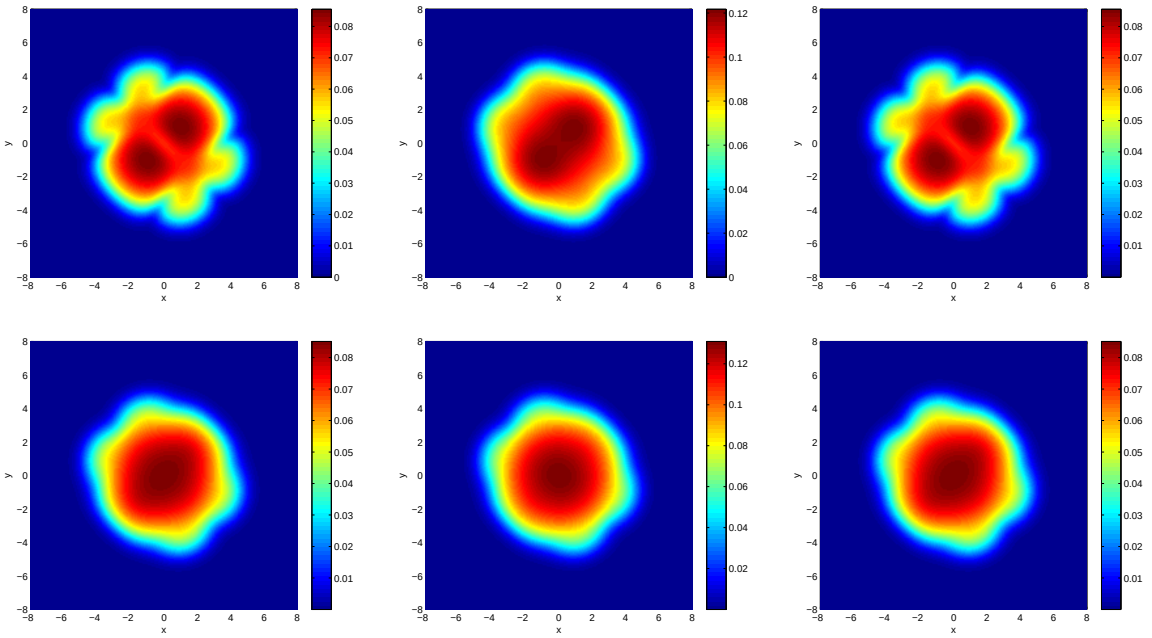

Figure 5: Ground states of ferromagnetic (top) and antiferromagnetic (bottom) spin-1 BECs with $B(x, y) = \sin(x) + \sin(y)$. From left to right: $|\phi_{1,g}|$, $|\phi_{0,g}|$ and $|\phi_{-1,g}|$. {*F5-1*}

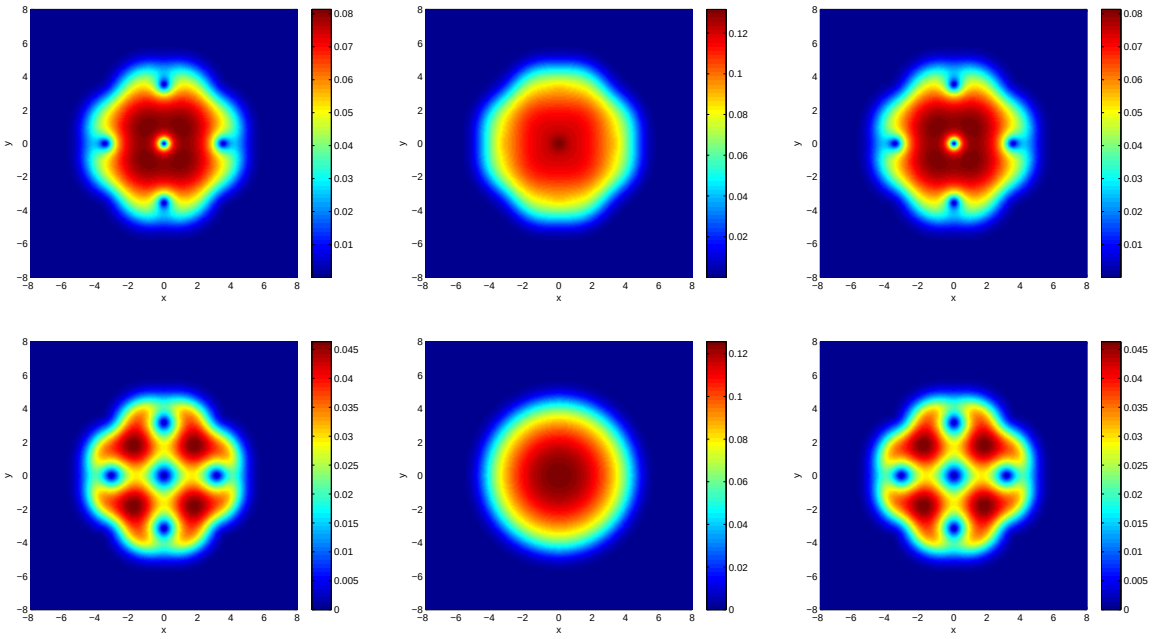

Figure 6: Ground states of ferromagnetic (top) and antiferromagnetic (bottom) spin-1 BECs with $B(x, y) = \sin(x) + i\sin(y)$. From left to right: $|\phi_{1,g}|$, $|\phi_{0,g}|$ and $|\phi_{-1,g}|$. {*F5-2*}

4.2.1 Comparison of different methods

{*section4-2-1*}

The numerical methods for computing ground states of spin-1 BECs in [5, 6, 17, 9] are computationally intensive, since they solve a coupled three-component system. In contrast,

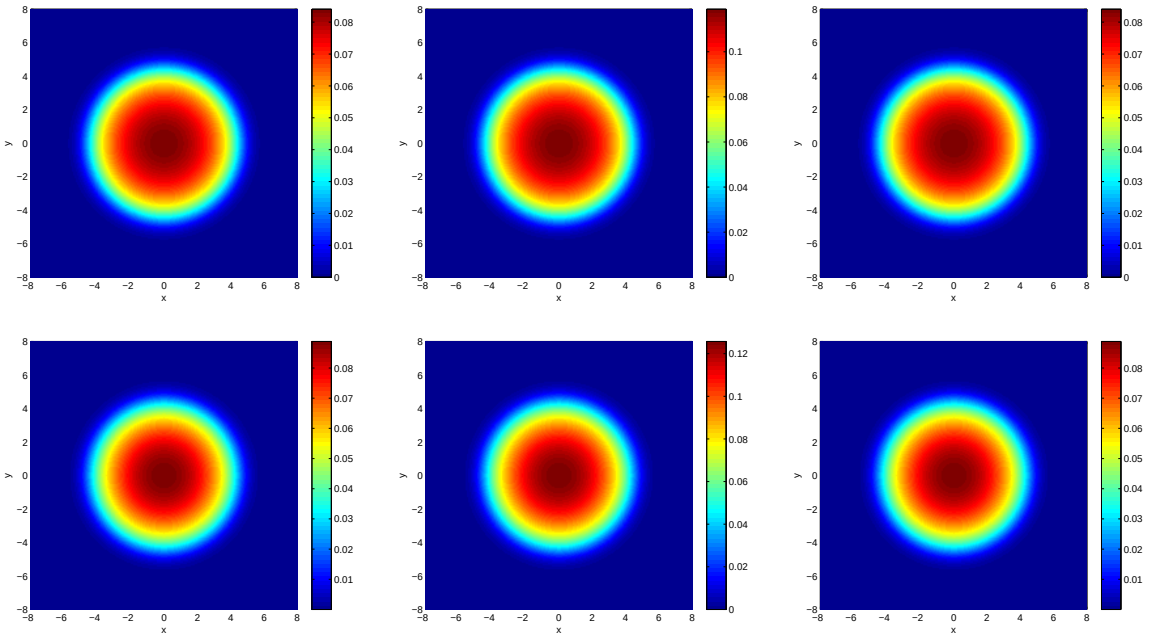

Figure 7: Ground states of ferromagnetic (top) and antiferromagnetic (bottom) spin-1 BECs with $B(x, y) = 1 + 2i$. From left to right: $|\phi_{1,g}|$, $|\phi_{0,g}|$ and $|\phi_{-1,g}|$. {F5-3}

our schemes introduced in Section 3 take into account the ferromagnetic or antiferromagnetic characterizations of the corresponding ground states and provide more efficient approaches for simulating the ground states in the case of $B(\mathbf{x}) \equiv 0$. To show their effectiveness, we compare our methods with that introduced in [6], which we will refer to as Bao-Lim's method for simplicity. Different methods are compared in terms of the ground state energy and the computing time.

In the following, we consider 1D cases, i.e. $d = 1$, and the external potential is chosen as $V_1(x) = x^2/2$. The problem is solved in a domain $[-32, 32]$ with $J = 2048$, i.e. the mesh size $\Delta x = 0.03125$. The time step is $\Delta t = 0.001$ in our simulations. We denote N as the total number of atoms and choose $N = 10000$ in the following examples. Since in ground states we have $M \leftrightarrow -M \Longleftrightarrow \phi_1 \leftrightarrow \phi_{-1}$, here we only present the results for $0 \leq M \leq 1$.

Example 3 We consider a ferromagnetic condensate with $\beta_n = 0.08716N$ and $\beta_s = -0.001748N$. The values of the interaction strengths β_n and β_s correspond to the experimental setup of ^{87}Rb confined in a cigar-shaped trapping potential with parameters as follows [21, 22, 25]: $m = 1.443 \times 10^{-25}$ kg, $\omega_x = 2\pi$ Hz, $\omega_y = \omega_z = 2\pi \times 20\pi\sqrt{2}$ Hz, $a_0 = 5.5$ nm $= 5.5 \times 10^{-9}$ m, and $a_2 = 5.182$ nm $= 5.182 \times 10^{-9}$ m. Correspondingly, the constant κ in the SMA formulation (3.10) is $\kappa = 0.085412N$.

For different magnetization $0 \leq M \leq 1$, we compare the ground state computed by our method based on the SMA in (3.6) and (3.9) and by Bao-Lim's method [6]. Figure 9 shows the density of each component in the ground states. Table 1 demonstrates the ground state energy and computing time spent by different methods. Note that here our motivation is to compare the speed of two methods in computing the ground states, and thus the

programs by different methods are run on the same computer. We understand that the time can be shortened if one uses an advanced computer or does parallel computations, which however is not our consideration here.

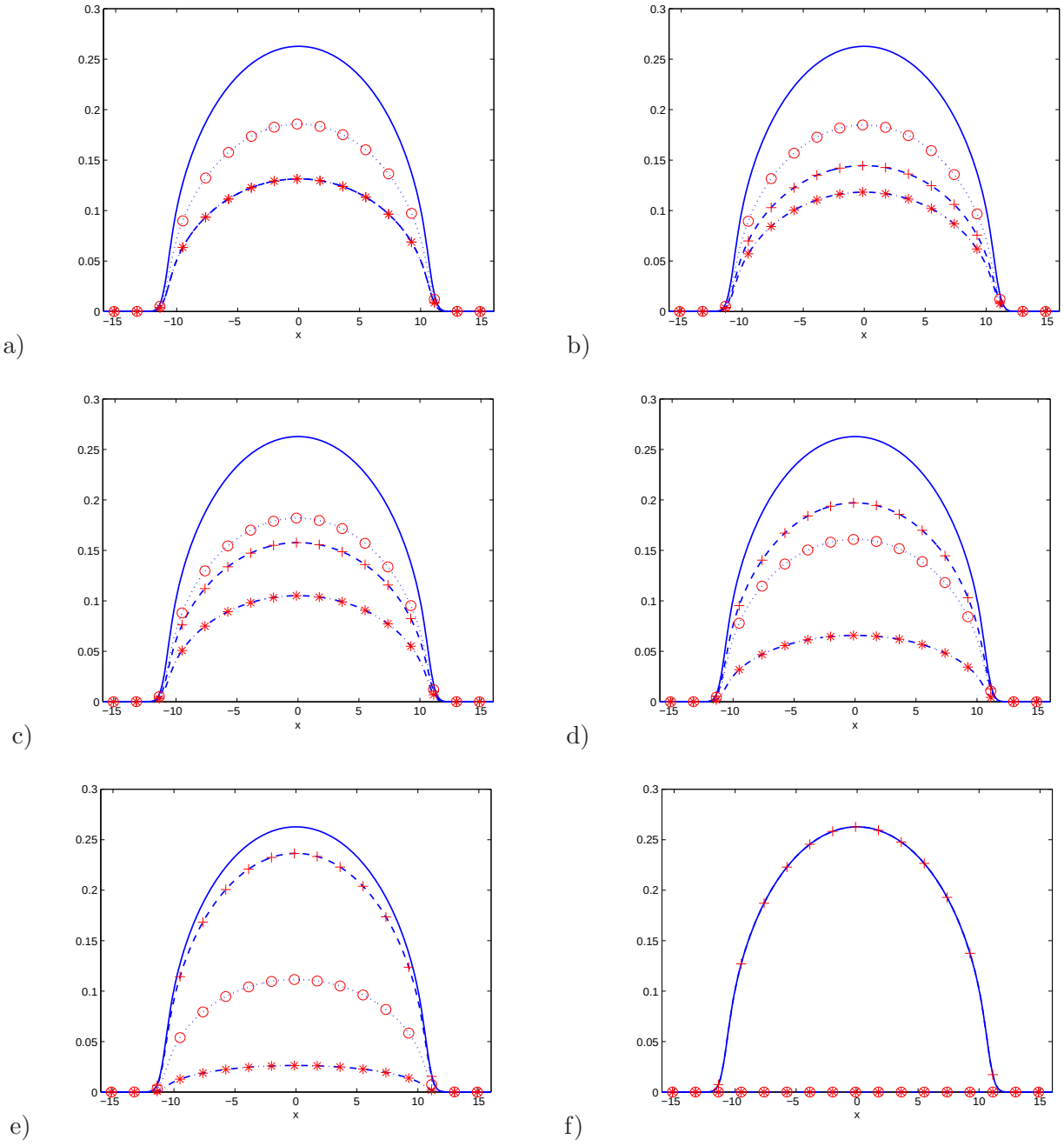

Figure 8: Ground states of the ferromagnetic spin-1 BECs in Example 3 computed by Bao-Lim's method ('+': $|\phi_{1,g}|$, 'o': $|\phi_{0,g}|$; '*': $|\phi_{-1,g}|$) and our method based on SMA (solid line: $u_g(x)$; dash line: $|\phi_{1,g}| = \gamma_1 u_g$; dot line: $|\phi_{0,g}| = \gamma_0 u_g$; dash-dot line: $|\phi_{-1,g}| = \gamma_{-1} u_g$ with γ_j given in (3.9)). From a) to f): M =0, 0.1, 0.2, 0.5, 0.8, 1. {F7}

M	Bao-Lim's method	Our method
0	132.9006	6.6544
0.1	145.1758	6.6544
0.2	223.4998	6.6544
0.3	271.1486	6.6544
0.4	288.8190	6.6544
0.5	282.1649	6.6544
0.6	259.8170	6.6544
0.7	239.0292	6.6544
0.8	166.8878	6.6544
0.9	119.0467	6.6544
Energy	$E_0(\Phi_g) = 35.4007$	$E_{\rm sma}(u_g) = 35.4007$

Table 1: Ground state energy and computing time by Bao-Lim's method [6] and our method in §3.1 for ferromagnetic condensates with different magnetizations $0 \le M \le 1$. {*T1*}

It shows in Fig. 9 that the ground states computed by our method agree with those by Bao-Lim's method for different magnetization M, where lines represent the results by our method and symbols represent those from Bao-Lim's method [6]. In addition, the ground state energies obtained from both methods are the same, which is independent of magnetization; see Table 1. However, the time spent by our method is much shorter (less than 6%) than that of Bao-Lim's method; see Table 1. Furthermore, the computing time by Bao-Lim's method [6] depends variously on the magnetization M.

Example 4 We consider an antiferromagnetic condensate with $\beta_n = 0.0241N$ and $\beta_s = 0.00075N$ in (1.1), which corresponds to $\chi = 0.02485N$ and $\nu = 0.02335N$ in the two-component reduction when $M \neq 0$. These values are based on the experimental setup of ^{23}Na confined in a cigar-shaped trapping potential with parameters as follows [21, 22, 25]: $m = 3.816 \times 10^{-26}$ kg, $\omega_x = 2\pi \times 20$ Hz, $\omega_y = \omega_z = 2\pi \times 400$ Hz, $a_0 = 2.646$ nm $= 2.646 \times 10^{-9}$ m, and $a_2 = 2.911$ nm $= 2.911 \times 10^{-9}$ m.

Similarly, we compare the ground states computed by these two methods in Figure 10 and the ground state energy and computing time for different magnetization $0 \le M \le 1$ are shown in Table 2. We see that for a fixed magnetization $M \neq 0$, the two methods obtain the identical ground states from both methods with $\phi_{0,g}(x) \equiv 0$. In addition, the ground state energy is also the same. However, Table 2 suggests that our method based on the two-component reduction is much faster than Bao-Lim's method [6] which solves a three-component system. Furthermore, even though our method solves a two-component GFDN, its computing time is less than a half of that used by Bao-Lim's method. Again, here our motivation is to compare the speed of these two methods. For this purpose, we run the programs of the two methods on the same computer and their computing time might be reduced if an advanced computer is used.

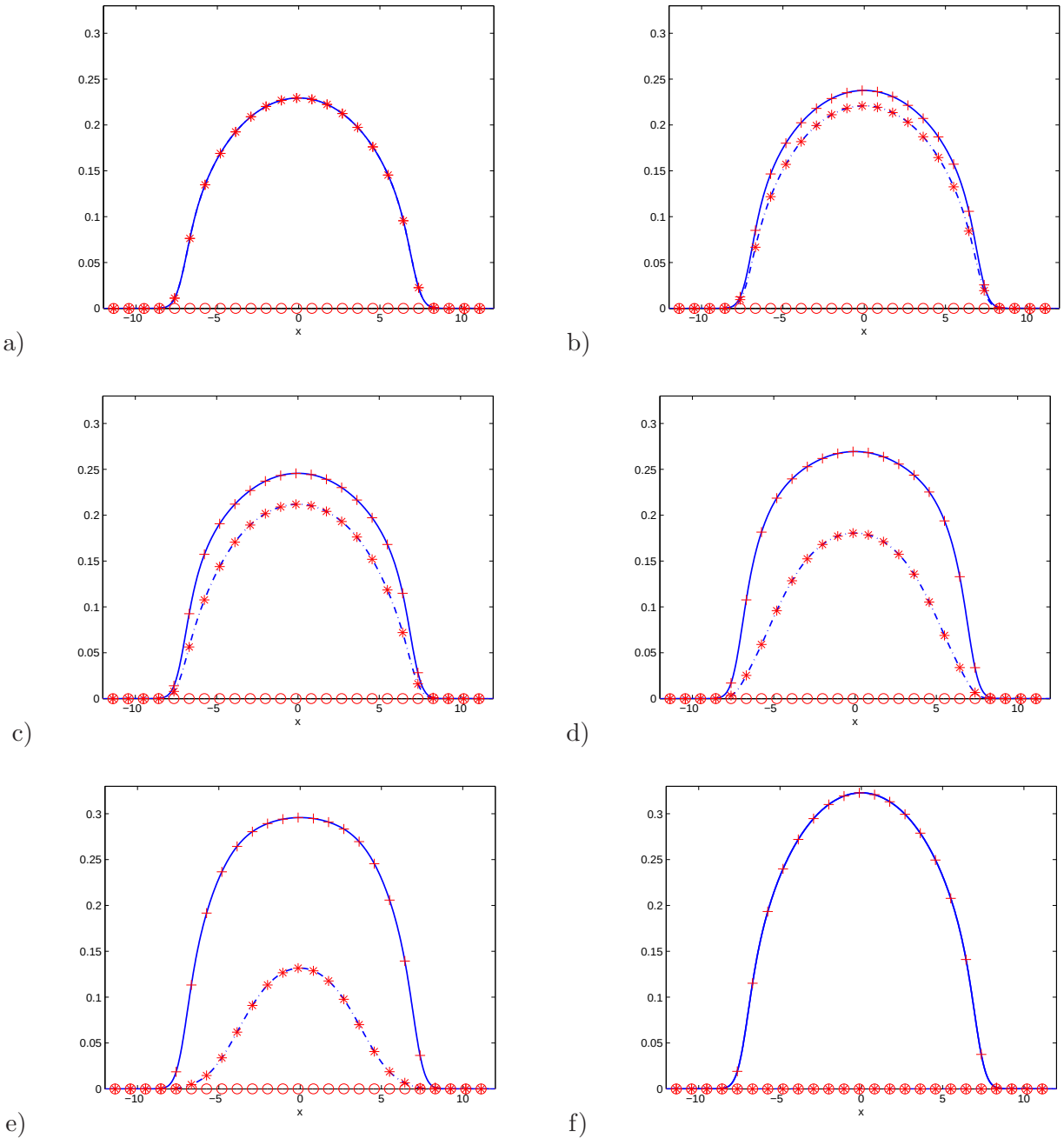

Figure 9: Ground states of the antiferromagnetic spin-1 BECs in Example 4 computed by Bao-Lim's method ('+': $|\phi_{1,g}|$, 'o': $|\phi_{0,g}|$; '*': $|\phi_{-1,g}|$) and our method based on the two-component reduction (solid line: $|\phi_{1,g}| = |u_{1,g}|$; dot line: $|\phi_{0,g}|$; dash-dot line: $|\phi_{-1,g}| = |u_{2,g}|$;). From a) to f): M =0, 0.1, 0.2, 0.5, 0.8, 1. {*F8*}

4.2.2 Applications of our methods

{*section4-2-2*}

In Section 4.2.1, we showed that our methods, based on the ferromagnetic or antiferromagnetic characterization of spin-1 BECs, obtain the same ground states as those by

	Bao-Lim's method		Our method	
M	Energy $E_0(\Phi_g)$	Computing time	Energy $E_{\rm tca}(\mathbf{u}_g)$	Computing time
0	15.2485	177.1892	15.2485	15.1419
0.1	15.2513	177.0494	15.2513	42.0558
0.2	15.2599	176.9190	15.2599	47.3362
0.3	15.2743	176.8998	15.2743	51.9579
0.4	15.2945	176.2563	15.2945	56.6422
0.5	15.3209	174.9268	15.3209	61.6046
0.6	15.3537	172.9923	15.3537	66.4197
0.7	15.3933	168.8066	15.3933	70.8586
0.8	15.4405	163.0863	15.4405	74.9606
0.9	15.4962	158.1879	15.4962	79.2583

Table 2: Ground state energy and computing time by Bao-Lim's method [6] and our method in §3.2 for antiferromagnetic condensates with different magnetization $0 \le M \le 1$. {*T2*}

Bao-Lim's method [6]. However, the computing time consumed by our methods is much less, which makes them more efficient in computing the ground states of spin-1 condensates when $B(\mathbf{x}) = 0$. In the following, we will apply our methods to study the ground states in different cases.

Example 5 We test the dependence of the ground state energy on the interaction constants β_n and β_s as well as on the magnetization M. To do this, 1D spin-1 BECs with a harmonic external potential $V_1(x) = x^2/2$ are considered. The computational domain is $[-32, 32]$ which is sufficiently large so that the truncation errors can be neglected. We choose the mesh size and time step as $\Delta x = 0.03125$ and $\Delta t = 0.001$, respectively. The following two cases are considered:

Case I. Ferromagnetic system with $\beta_s < 0$. Figure 10 (top) shows the ground state energy with respect to different interaction constants β_n and β_s and different magnetization M. It suggests that the energy monotonically increases with $\beta_n + \beta_s$ increasing, but it is independent of the magnetization M. Furthermore when $\beta_n + \beta_s$ is large, the ground state energy of a ferromagnetic spin-1 condensate can be approximated by the Thomas-Fermi energy of its SMA counterpart, i.e.,

$$E_{0,g} \approx E^{\rm TF}_{{\rm sma},g} = \frac{3}{10}\left(\frac{3\kappa\omega_x}{2}\right)^{\frac{2}{3}}, \qquad (4.1) \quad \{\}$$

where ω_x is the trapping frequency in x-direction and in this example, we use $\omega_x = 1$.

Case II. Antiferromagnetic system with $\beta_s > 0$. Figure 10 (bottom) shows the ground state energy for different parameters β_n, β_s and M. Different from that in ferromagnetic cases, the ground state energy in an antiferromagnetic system depends on the constants $\beta_n + \beta_s$, $\beta_n - \beta_s$ and the magnetization M. For fixed $\beta_n \pm \beta_s$, the ground state energy increases when the magnitude of M, i.e., $|M|$, increases, and the energy reaches its minimizer at $M = 0$; see Fig. 10 (bottom, right).

Example 6 We apply our methods to study the ground states of 2D spin-1 condensates.

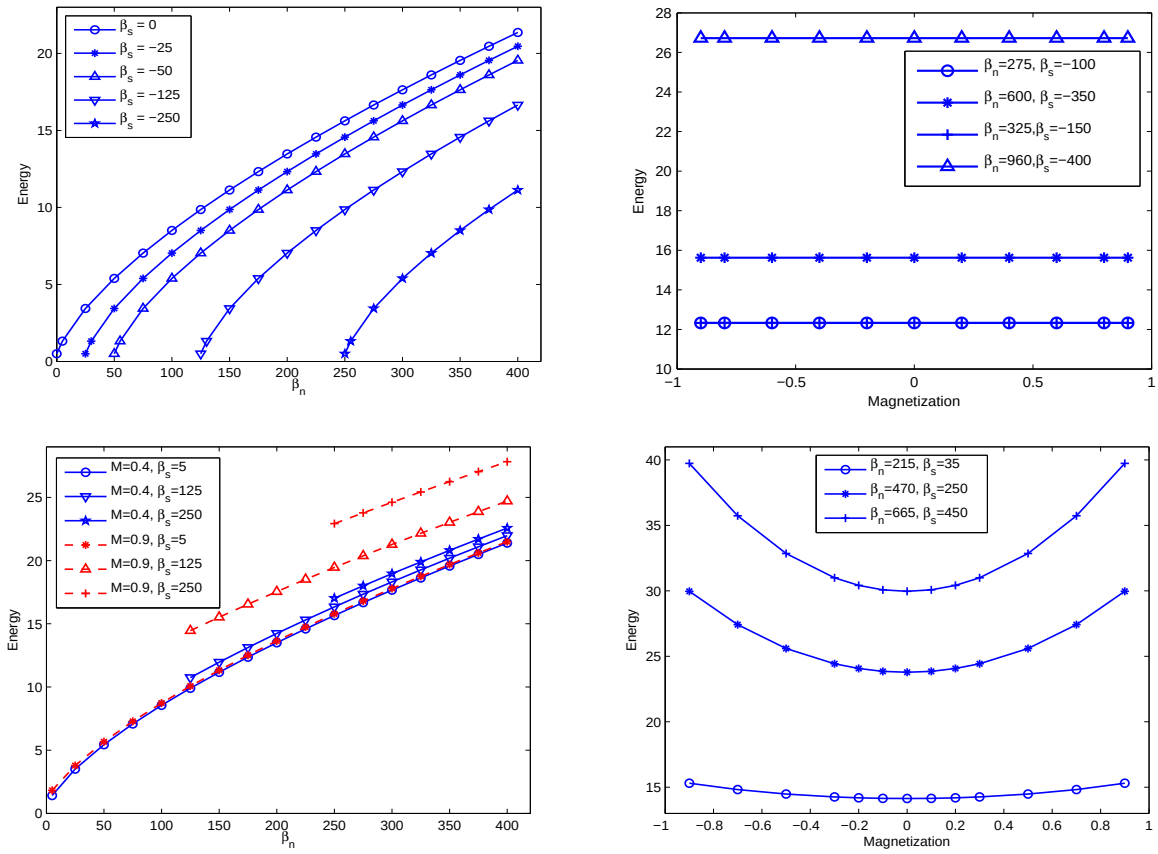

Figure 10: Energy versus the interaction constants β_n and β_s (left) and the magnetization M (right) in ferromagnetic (top) and antiferromagnetic (bottom) spin-1 condensates. {*F9*}

The following two types of external potentials are considered: (i) harmonic potential $V_2(\mathbf{x}) = (\omega_x^2 x^2 + \omega_y^2 y^2)/2$; (ii) isotropic harmonic potential plus an optical lattice, i.e.,

$$V_2(\mathbf{x}) = \frac{1}{2}(x^2 + y^2) + 10\left[\sin(\kappa_x x)^2 + \sin(\kappa_y y)^2\right], \tag{4.2}$$ {*optical*}

where $\kappa_x, \kappa_y > 0$ are two constants. Then we study the ground states of

Case I. Ferromagnetic system with $\beta_n = 560$ and $\beta_s = -100$ and $M = 0.5$.

Case II. Antiferromagnetic system with $\beta_n = 300$, $\beta_s = 100$ and $M = 0.5$.

Figure 11 presents the density of ground state calculated from the single-mode reduction for ferromagnetic cases, and the ground states of the corresponding spin-1 BECs can be obtained by using (3.6) and (3.9) with $M = 0.5$. Figure 12 shows the ground states of antiferromagnetic spin-1 condensates, where only $|\phi_{1,g}| = |u_{1,g}|$ and $|\phi_{-1,g}| = |u_{2,g}|$ are presented since $|\phi_{0,g}| \equiv 0$ in this case. Numerical simulations show that our methods based on the single-mode and two-component reduction are dramatically faster than the Bao-Lim method [6] in higher dimensional cases.

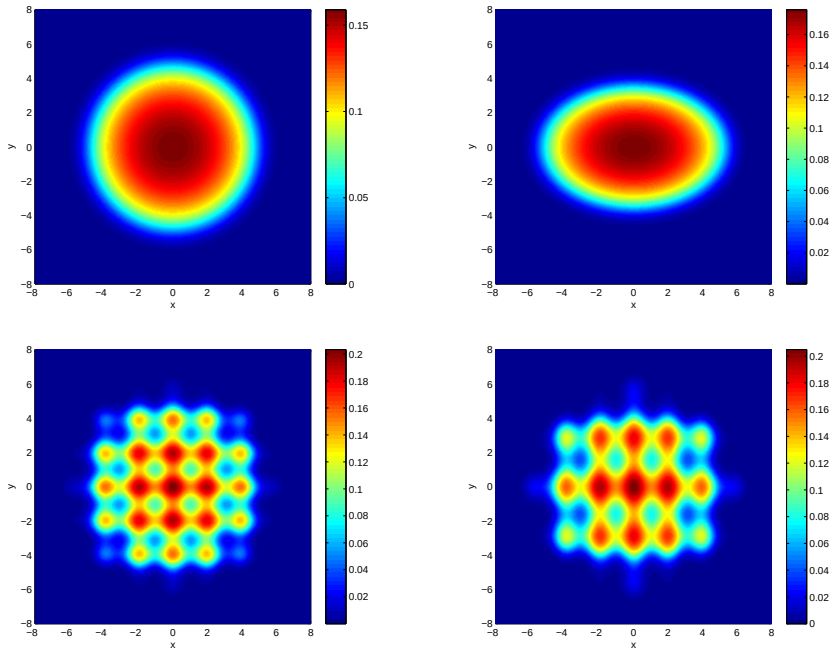

Figure 11: Ground states of 2D ferromagnetic spin-1 BECs in Example 6 with a harmonic trap (top: $\gamma_x = \gamma_y = 1$ (left); $\gamma_x = 1$ and $\gamma_y = 1.5$ (right)) and a harmonic plus optical lattice potential (bottom: $\kappa_x = \kappa_y = \frac{\pi}{2}$ (left); $\kappa_x = \frac{\pi}{2}$ and $\kappa_y = \frac{\pi}{3}$ (right)). {*F10*}

5 Conclusions

{*section5*}

We proposed efficient and simpler numerical methods for computing the ground states of spin-1 BEC with/without the Ioffe-Pritchard magnetic field $B(\mathbf{x})$. Noticing that there have been no numerical studies on the ground state of spin-1 BECs with $B(\mathbf{x}) \neq 0$, we first introduced a numerical method for it. Then our methods were applied to study the ground states in both 1D and 2D cases. Our numerical results suggested that when $B(\mathbf{x}) \neq 0$, the $m_F = \pm 1$ components in the ground states always have the same density functions, which implies that the stationary states with the magnetization $M = 0$ have the lowest energy. In particular, if $B(\mathbf{x}) \equiv B$ is a constant, the ground states satisfy the single-mode reduction given in (3.6) with the constants $\gamma_{\pm 1} = \frac{1}{2}$ and $\gamma_0 = \frac{\sqrt{2}}{2}$ exactly. We will leave its rigorous mathematical justifications for future work.

On the other hand, when $B(\mathbf{x}) = 0$, we took into account the ferromagnetic or antiferromagnetic characterizations of the ground states, which results in efficient numerical methods for computing the ground state. In the ferromagnetic cases, the ground state can be always described exactly by the single-mode approximation. While in the antiferromagnetic systems, the situations can be classified into two types: (i) when $M \neq 0$, the $m_F = 0$ component becomes zero in the ground states so that the spin-1 BECs can be characterized by a two-component reduction; (ii) if $M = 0$, the ground states satisfy the SMA as in the ferromagnetic systems, but the constants are not unique. Considering these properties of the ground states, we proposed numerical methods to compute the ground state of the reduced single-mode or two-component systems. Then the ground states of the original spin-1 condensates can be obtained from those of the reduced systems. Nu-

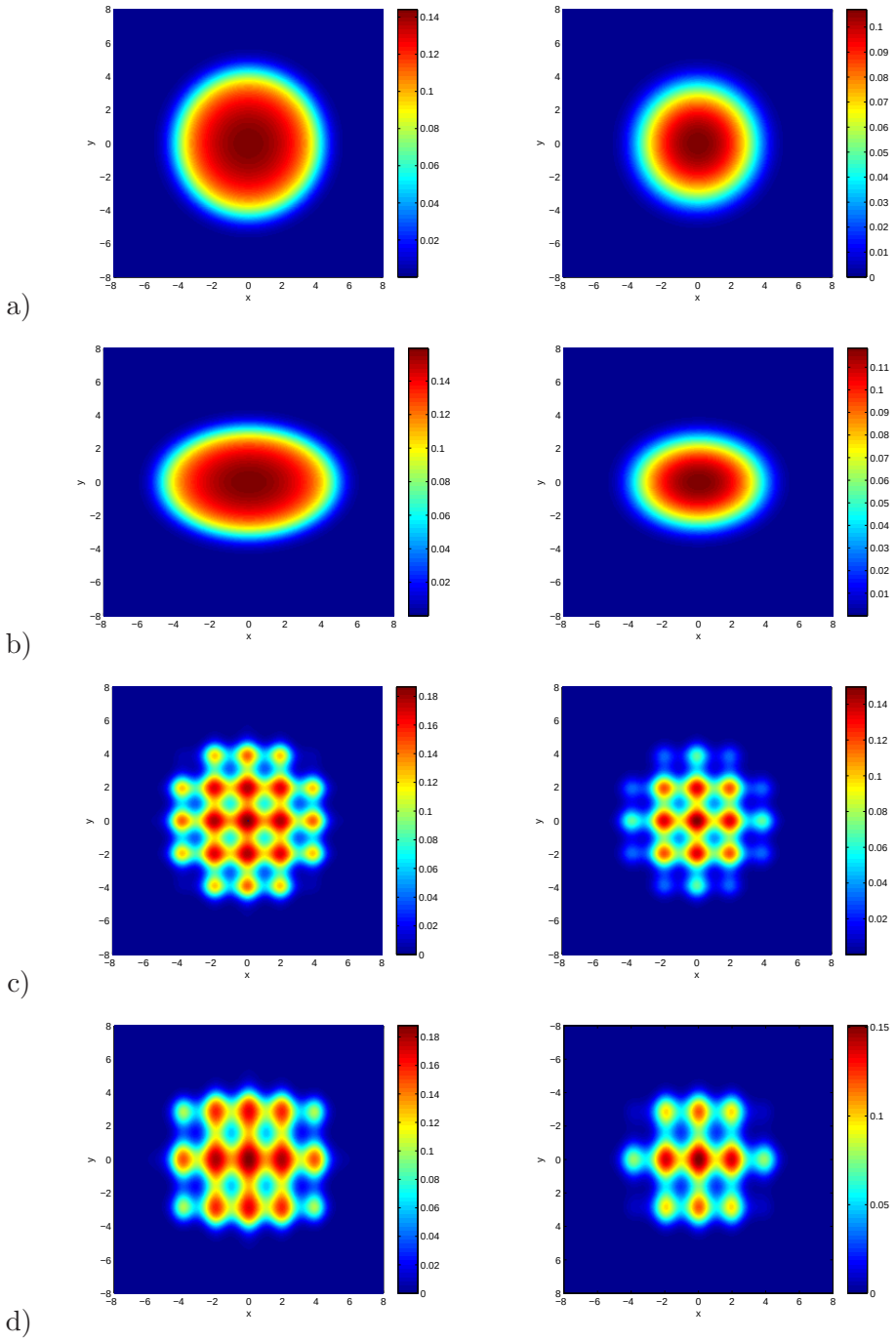

Figure 12: Ground states of 2D antiferromagnetic spin-1 BECs in Example 6 with a harmonic trap (top: $\gamma_x = \gamma_y = 1$ (a); $\gamma_x = 1$ and $\gamma_y = 1.5$ (b)) and a harmonic plus optical lattice potential (bottom: $\kappa_x = \kappa_y = \frac{\pi}{2}$ (c); $\kappa_x = \frac{\pi}{2}$ and $\kappa_y = \frac{\pi}{3}$ (d)). {*F11*}

merical results suggested that our methods give the same results as those by Bao-Lim's method in [6]. However, the computing time used by our methods is much shorter. In addition, we apply our methods to study the relation between the ground state energy

and the interaction parameters β_n, β_s as well as the magnetization M.

Acknowledgement W. B. acknowledges support from the Academic Research Fund of Ministry of Education of Singapore grant R-146-000-120-112. I. C. thanks support from the National Science Council of the Republic of China (Grant 99-2115-M-002-003-MY3). Y. Z. thanks support by the University of Missouri Research Board and the Simons Foundation (Award No. 210138). Part of this work was done when the authors were visiting the Institute for Mathematical Sciences at the National University of Singapore in 2012.

References

[1] M.H. Anderson, J.R. Ensher, M.R. Matthews, C.E. Wieman and E.A. Cornell, Observation of Bose–Einstein condensation in a dilute atomic vapor, Science, **269** (1995), pp. 198–201.

[2] W. Bao and Q. Du, Computing the ground state solution of Bose–Einstein condensates by a normalized gradient flow, SIAM J. Sci. Comput., **25** (2004), pp. 1674–1697.

[3] W. Bao, Q. Du and Y. Zhang, Dynamics of rotating Bose–Einstein condensates and their efficient and accurate numerical computation, SIAM J. Appl. Math., **66** (2006), pp. 758–786.

[4] W. Bao, I.-L. Chern and F.Y. Lim, Efficient and spectrally accurate numerical methods for computing ground and first excited states in Bose–Einstein condensates, J. Comput. Phys., **219** (2006), pp. 836–854.

[5] W. Bao and H. Wang, A mass and magnetization conservative and energy-diminishing numerical method for computing ground state of spin-1 Bose–Einstein condensates, SIAM J. Numer. Anal., **45** (2007), pp. 2177–2200.

[6] W. Bao and F.Y. Lim, Computing ground states of spin-1 Bose–Einstein condensates by the normalized gradient flow, SIAM J. Sci. Comput., **30** (2008), pp. 1925–1948.

[7] W. Bao and Y. Zhang, Dynamical laws of the coupled Gross–Pitaevskii equations for spin-1 Bose–Einstein condensates, Meth. Appl. Anal., **17** (2010), pp. 49–80.

[8] D. Cao, I.-L. Chern and J.-C. Wei, On ground states of spinor Bose–Einstein condensates, Nonlinear Differ. Equ. Appl., **18** (2011), pp. 427–445.

[9] J.-H. Chen, I.-L. Chern and W. Wang, Exploring ground states and excited states of spin-1 Bose–Einstein condensates by continuation methods, J. Comput. Phys., **230** (2011), pp. 2222–2236.

[10] M.L. Chiofalo, S. Succi and M.P. Tosi, Ground state of trapped interacting Bose–Einstein condensates by an explicit imaginary-time algorithm, Phys. Rev. E, **62** (2002), pp. 7438-7444.

[11] K.B. Davis, M.O. Mewes, M.R. Andrews, N.J. van Druten, D.S. Durfee, D.M. Kurn and W. Ketterle, Bose–Einstein condensation in a gas of sodium atoms, Phys. Rev. Lett., **75** (1995), pp. 3969–3973.

[12] U. Ernst, A. Marte, F. Schreck, J. Schuster and G. Rempe, Bose–Einstein condensation in a pure Ioffe-Pritchard field configuration, Euro. phys. Lett., **41** (1998), pp. 1–6.

[13] T.-L. Ho and S.K. Yip, Fragmented and single condensate ground states of spin-1 bose gas, Phys. Rev. Lett., **84** (2000), 4031–4034.

[14] T. Isoshima, M. Nakahara, T. Ohmi and K. Machida, Creation of a persistent current and vortex in a Bose–Einstein condensate of alkali-metal atoms, Phys. Rev. A, **61** (2000), article 063610.

[15] C.K. Law, H. Pu and N.P. Bigelow, Quantum spins mixing in spinor Bose–Einstein condensates, Phys. Rev. Lett., **81** (1998), pp. 5257–5261.

[16] A.E. Leanhardt, Y. Shin, D. Kielpinski, D.E. Prichard and W. Ketterle, Coreless vortex formation in a spinor Bose-Einstein condensate, **90** (2003), article 140403.

[17] F.Y. Lim and W. Bao, Numerical methods for computing the ground state of spin-1 Bose–Einstein condensates in a uniform magnetic field, Phys. Rev. E, **78** (2008), article 066704.

[18] L. Lin and I.-L. Chern, Characterization of the ground states of spin-1 Bose-Einstein condensates, arXiv:1102.0832v2.

[19] M. Matuszewski, T.J. Alexander and Y.S. Kivshar, Excited spin states and phase separation in spinor Bose–Einstein condensates, Phys. Rev. A, **80** (2009), article 023602.

[20] M. Matuszewski, Ground states of trapped spin-1 condensates in magnetic field, Phys. Rev. A, **82** (2010), article 053630.

[21] H.J. Miesner, D.M. Stamper-Kurn, J. Stenger, S. Inouye, A.P. Chirkkatur and W. Ketterle, Observation of metastable states in spinor Bose–Einstein condensates, Phys. Rev. Lett., **82** (1999), pp. 2228–2231.

[22] T. Mizushima, N. Kobayashi and K. Machida, Coreless and singular vortex lattices in rotating spinor Bose–Einstein condensates, Phys. Rev. A, **70** (2004), article 043613.

[23] K. Murata, H. Saito and M. Ueda, Broken-axisymmetry phase of a spin-1 ferromagnetic Bose–Einstein condensate, Phys. Rev. A, **75** (2007), article 013607.

[24] H. Pu, C.K. Law, S. Raghavan, J.H. Eberly and N. P. Bigelow, Spin-mixing dynamics of a spinor Bose–Einstein condensate, Phys. Rev. A, **60** (1999), pp. 1463–1470.

[25] D.M. Stamper-Kurn and W. Ketterle, Spinor condensates and light scattering from Bose–Einstein condensates, in Proceedings of Les Houches 1999 Summer School (Session LXXII), **72** (2001), pp. 139–217.

[26] J. Stenger, S. Inouye, D.M. Stamper-Kurn, H.-J. Miesser, A.P. Chikkatur and W. Ketterle, Spin domains in ground state spinor Bose–Einstein condensates, Nature, **396** (1998), pp. 345-348.

[27] T. Swislocki and M. Matuszewski, Controlled creation of spin domains in spin-1 Bose–Einstein condensates by phase separation, Phys. Rev. A, **86** (2012), article 023601.

[28] M. Ueda and Y. Kawaguchi, Spinor Bose–Einstein condensates, arXiv:1001.2072v2.

[29] K.C. Wright, Stimulated Raman interactions in a spinor Bose–Einstein condensate, Ph.D. thesis, University of Rochester, (2009).

[30] S. Yi, Ö.E. Müstecaplioglu, C.P. Sun and L. You, Single-mode approximation in a spinor-1 atomic condensate, Phys. Rev. A, **66** (2002), article 011601.

[31] R. Zeng and Y. Zhang, Efficiently computing vortex lattices in fast rotating Bose–Einstein condensates, Comput. Phys. Commun., **180** (2009), pp. 854-860.